were: *ZIP6*, 5′-TCTGTCACAAATCCCCTTCA-3′ (sense), 5′-GGAGGGCTCTTGTGAGTCTG-3′ (antisense); *ZIP10*, 5′-CCTGGTTCCTGAAGATGAGG-3′ (sense), 5′-CATGGCAGAGAGGAGGTTGT-3′ (antisense); *E-CADHERIN*, 5′-GTCATTGAGCCTGGCAATTT-3′ (sense), 5′-GCTTGAACTGCCGAAAAATC-3′ (antisense); *VIMENTIN*, 5′-CCTTGAACGCAAAGTGGAAT-3′ (sense), 5′-GCTTCAACGGCAAAGTTCTC-3′ (antisense); *GAPDH*, 5′-TGAAGGTCGGAGTCAACGGAT-3′ (sense), 5′-CATGTGGGCCATGAGGTCCAC-3′ (antisense).

RNA interference. The small interfering RNA (siRNA) for human *ZIP6*, human *ZIP10* and the control (siCONTROL non-targeting siRNA #1) were obtained from Dharmacon Inc., Chicago, IL, USA. The target sequences of the siRNA for human *ZIP6* were 5′-GAAGUUAUCUGUAAUCUUGUU-3′, 5′-GAAGUGACCUCAACUGUGUUU-3′, 5′-UGAAGGAACUCACUUUCUAUU-3′ and 5′-UGACUUUGCUGUUCUACUAUU-3′. For human *ZIP10* they were 5′-GAACGUCACUCAGUUAUUAUU-3′, 5′-GGAAGAAUAUGAUGCUGUAUU-3′, 5′-CCACAAACCUGAUCGUGUAUU-3′ and 5′-GAAAGGACUUGUUGCUCUAUU-3′. Cells were treated with a mixture of all four oligonucleotides, following the manufacturer's protocol, 24 h before the zinc uptake or cell migration assays.

Zinc assays. To chelate intracellular Zn, Cu, Fe, or Mn, 10 μM *N,N,N′,N′*-tetrakis(2-pyridylmethyl)ethylenediamine (TPEN; Molecular Probes, Eugene, OR, USA) 10 μM disodium bathocuproine disulfonate (BCDS; Sigma-Aldrich, St. Louis, MO, USA), 10 μM 2,2′-dipyridyl disulfonate (Sigma-Aldrich, St. Louis, MO, USA), or 10 μM sodium para-aminosalicylic acid disulfonate (PAS; Sigma-Aldrich), respectively, was added to the culture medium 24 h prior to observation. To rescue the zinc level, 5 μM $ZnCl_2$ or 1 μM pyrithione was added to the TPEN-containing medium. For the ^{65}Zn uptake assays, the cells were grown to 50% confluence, incubated at 37°C for the indicated times in DMEM and 0.1 μM $^{65}ZnCl_2$ (Oak Ridge National Laboratory, Oak Ridge, IN, USA), washed three times with phosphate-buffered saline, and then harvested. Cell-associated radioactivity was measured with a Packard Auto-Gamma 5650 counter.

***In vitro* transwell migration assay and time-lapse imaging.** *In vitro* transwell migration assays were carried out using 5.0-μm pore size Costar Transwell inserts (Corning Inc., Lowell, MA, USA), according to the manufacturer's protocol. To each well was added 2×10^4 cells, which were incubated in the presence of 10% FBS for 24 h. Cells that migrated to the bottom of the transwell membrane were fixed with methanol, stained with hematoxylin and eosin, and counted under a microscope. Time-lapse images were obtained every 20 min under the indicated conditions. Migration rates (mean ± 1 SD [μm/min]) were calculated from 20 independent cells in each experiment.

Statistical analysis. Differences in expression levels of ZIP6 and ZIP10 mRNA between various subgroups were evaluated using Student's *t*-test.

Results

Correlation of high ZIP10 mRNA expression with lymph node metastasis in clinical breast cancers. We investigated whether *ZIP6* and *ZIP10* expression correlated with certain clinicopathological phenotypes of clinical breast tumor samples by real-time PCR (Table 1; Fig. 1). We observed a significantly higher level of *ZIP10* transcript in the lymph node metastasis-positive group compared with the metastasis-negative group ($P = 0.00080$) (Table 1; Fig. 1b), whereas no significant difference in the *ZIP6* transcript was seen ($P = 0.94$) (Fig. 1a). High *ZIP6* mRNA expression was associated with better prognostic parameters, such as better histological grade (I or II) ($P < 0.00001$), estrogen receptor positivity ($P < 0.0001$) and HER2 negativity ($P < 0.0001$) (Table 1), consistent with previous findings that *ZIP6* expression is estrogen regulated and not associated with malignant phenotypes in clinical breast cancer.[16] These clinical findings suggested that the zinc transporter ZIP10 is more likely than ZIP6 to correlate with cancer invasion and metastasis.

Table 1. Relationship between the clinicopathological parameters and ZIP6 or ZIP10 mRNA expression in breast cancer tissues

Parameter	Total $n = 177$	*ZIP6* mean ± SD ($\times 10^{-3}$)	*ZIP10* mean ± SD ($\times 10^{-5}$)
Tumor size			
≤2 cm	66	6.43 ± 9.61	4.76 ± 5.26
>2 cm	109	6.63 ± 8.85	6.63 ± 5.56
Unknown	2		
Histological grade			
I, II	131	7.82 ± 9.88*	6.42 ± 5.56
III	38	1.88 ± 3.73	4.20 ± 5.51
Unknown	8		
Lymph node metastasis			
Negative	92	6.44 ± 9.32	4.51 ± 4.87***
Positive	85	6.55 ± 8.87	7.29 ± 5.87
Unknown	0		
Estrogen receptor			
Positive	104	8.51 ± 9.28**	6.55 ± 5.59
Negative	68	3.03 ± 6.64	4.67 ± 5.34
Unknown	5		
Progesterone receptor			
Positive	84	7.85 ± 8.21	6.76 ± 5.90
Negative	88	4.91 ± 9.03	4.89 ± 5.07
Unknown	5		
HER2 status			
Negative	81	7.19 ± 9.82**	5.18 ± 5.06
Positive	17	1.81 ± 2.83	4.01 ± 4.11
Unknown	79		

Age range: 28–87 years (mean = 54 years). *$P < 0.00001$, **$P < 0.0001$, ***$P < 0.001$ (Student's *t*-test).

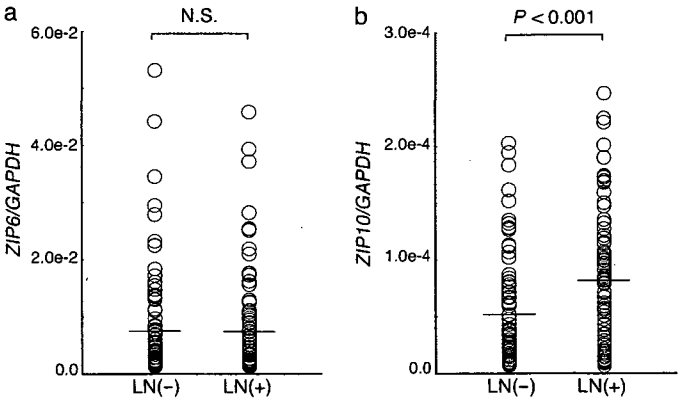

Fig. 1. mRNA expression of ZIP6 and ZIP10 in clinical breast cancers. The mRNA expression of (a) *ZIP6* and (b) *ZIP10* was evaluated by quantitative real-time polymerase chain reaction analysis in lymph-node metastasis-negative (LN–), and -positive (LN+) breast cancers. The bar indicates the mean value.

Correlation of high ZIP10 mRNA expression with the invasive phenotype of breast cancer cell lines. To test whether zinc transporters are involved in the metastatic phenotype of breast cancer cells, we analyzed the mRNA expression of the *ZIP* (*ZIP1–14*), which mediate zinc influx into the cytosol[10] in several breast cancer cell lines. These included the invasive and metastatic breast cancer cell lines MDA-MB-231 and MDA-MB-435S, which express low E-cadherin and high vimentin, and the less metastatic

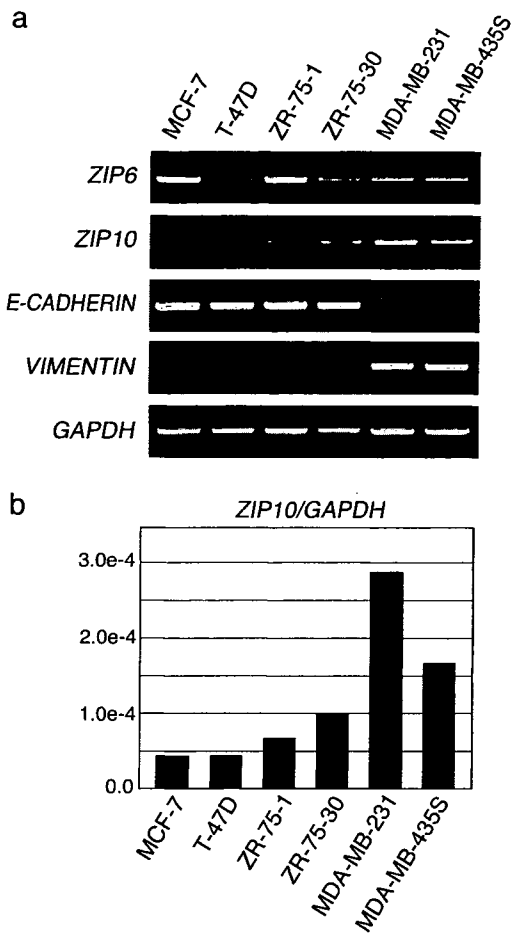

Fig. 2. mRNA expression of ZIP10 in breast cancer cell lines. (a) mRNA expression of *ZIP6*, *ZIP10*, *E-CADHERIN*, and *VIMENTIN* was evaluated by semiquantitative reverse transcription polymerase chain reaction (PCR) in less metastatic breast cancer cell lines (MCF7, T47-D, ZR75-1, ZR75-30) and highly metastatic lines (MDA-MB-231 and MDA-MB-435S), and (b) the relative mRNA expression of *ZIP10* in these six breast cancer cell lines was evaluated by real-time PCR.

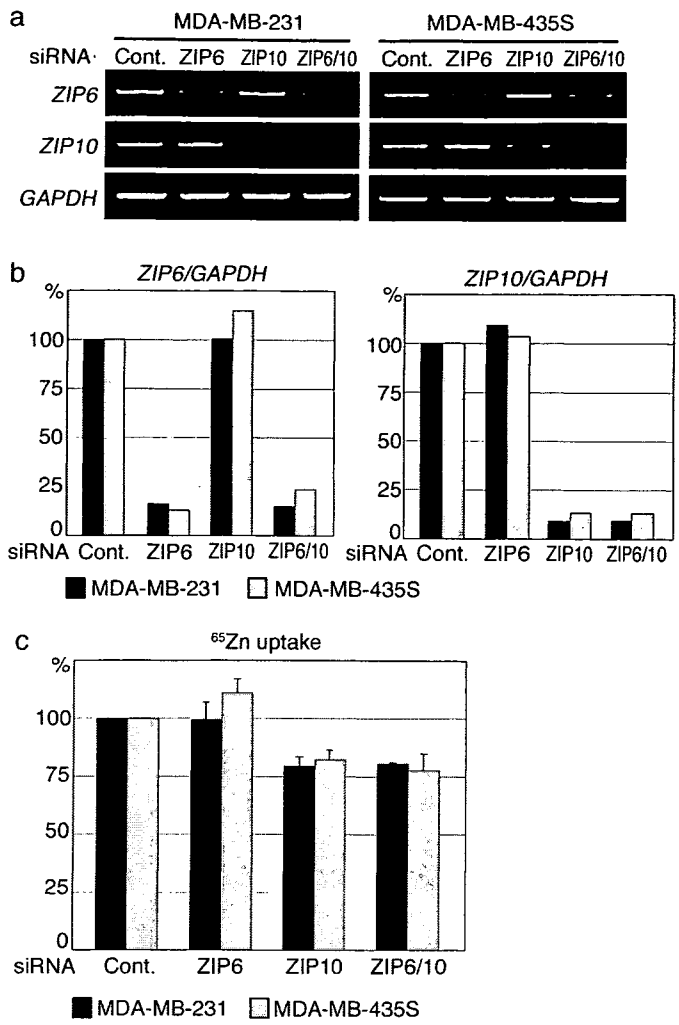

Fig. 3. ZIP10 mRNA expression and ^{65}Zn uptake of MDA-MB-231 and MDA-MB-435S cells expressing control, ZIP6, ZIP10 or ZIP6/ZIP10 small interfering RNA (siRNA). (a) Semiquantitative reverse transcription polymerase chain reaction (PCR) and (b) real-time PCR showed the knockdown effect of ZIP6 siRNA and/or ZIP10 siRNA. (c) Relative zinc uptake activity was evaluated by the counts per minute (CPM) of cells incubated with the ^{65}Zn isotope. Each figure shows a representative result of at least three experiments.

breast cancer cell lines MCF-7, T-47D, ZR-75-1 and ZR-75-30. Among the ZIP zinc transporters we screened, the expression of *ZIP10* was relatively upregulated in the highly metastatic cell-lines MDA-MB-231 and MDA-MB-435S (Fig. 2a), which we confirmed by real-time PCR (Fig. 2b), whereas the expression of *ZIP6* was not. These results also suggest that ZIP10 may be a major ZIP that regulates human breast cancer progression.

ZIP10 is essential for the invasive behavior of MDA-MB-231 and MDA-MB-435S breast cancer cells *in vitro*. To examine whether ZIP6 or ZIP10 is involved in breast cancer progression, we generated ZIP6-, ZIP10- and ZIP6/10-knockdowns and control MDA-MB-231 and MDA-MB-435S cells using siRNA for human *ZIP6*, human *ZIP10* and the control. Reverse transcription–PCR and real-time PCR analyses of these MDA-MB-231 and MDA-MB-435S knockdown cells showed that mRNA expression of *ZIP6* and *ZIP10* was specifically depleted by each siRNA in both cell types (Fig. 3a,b). In a transwell migration assay, the control and ZIP6-knockdown MDA-MB-231 cells exhibited high migration activity, which was inhibited by ZIP10 or ZIP6/10 depletion (Fig. 4a). Time-lapse analysis of these cells also highlighted their requirement for ZIP10 in their migratory behavior (Fig. 4c,d). Control and ZIP6-knockdown MDA-MB-231 cells showed active migration, reflecting their invasive property, whereas ZIP10- and ZIP6/10-knockdown MDA-MB-231 cells exhibited poor migratory activity. Similar results were obtained using MDA-MB-435S cells (Fig. 4a,c,d). These results indicated that ZIP10, but not ZIP6, is involved in the migratory activity of these breast cancer cells, and suggested that zinc transported via ZIP10 has essential regulatory functions in this activity.

Zinc is essential for the invasive behavior of MDA-MB-231 and MDA-MB-435S breast cancer cells *in vitro*. Because ZIP6 and ZIP10 belong to the ZIP zinc-transporter family, whose members are thought to mediate zinc influx into the cytosol, we carried out a ^{65}Zn uptake assay using the knockdown cells. ZIP10- and ZIP6/10-knockdown MDA-MB-231 or MDA-MB-435S cells incorporated significantly less ^{65}Zn than their respective controls and ZIP6-knockdown cells (Fig. 3c). This indicated that ZIP10 was involved in the zinc uptake of MDA-MB-231 or MDA-MB-435S breast cancer cells, whereas ZIP6-knockdown had no significant effect on zinc uptake in these cells, and suggested that zinc transported by ZIP10 might be involved in the migratory activity of these cells. To examine whether zinc is

doi: 10.1111/j.1349-7006.2007.00446.x

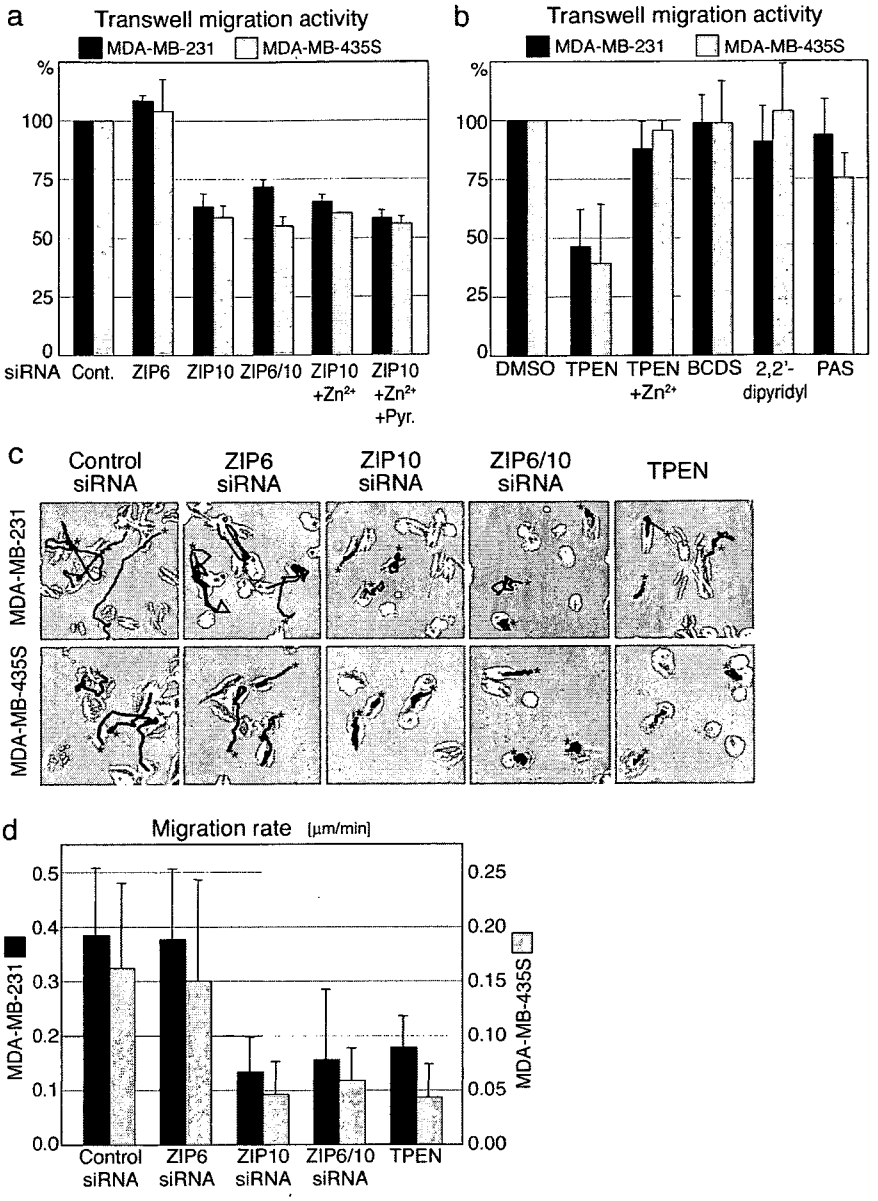

Fig. 4. The effects of ZIP10 knockdown on cancer cell migration. (a) MDA-MB-231 and MDA-MB-435S cells expressing control, ZIP6, ZIP10 or ZIP6/ZIP10 small interfering RNA (siRNA) were incubated with or without 5 μM ZnCl2 (Zn^{2+}) or 1 μM zinc pyrithione (pyr), for 24 h during *in vitro* transwell migration assays. (b) MDA-MB-231 and MDA-MB-435S cells were incubated with dimethylsulfoxide (control), 10 μM TPEN, 10 μM TPEN + 5 μM $ZnCl_2$ (Zn^{2+}), 10 μM disodium bathocuproine disulfonate (BCDS), 10 μM 2,2'-dipyridyl, or 10 μM sodium para-aminosalicylic acid (PAS) for 24 h during *in vitro* transwell migration assays. Error bars represent the standard deviations for three replicates. (c) The migratory tracks of individual cells were obtained by time-lapse imaging and (d) the migration rate (μm/min) over a 24-h incubation period was calculated. Cells expressing control, ZIP6, ZIP10 and ZIP6/10 siRNA were incubated without TPEN, and those expressing control siRNA were incubated with TPEN. Three views of representative migratory tracks from each condition are shown in panel (c). Lines and asterisks represent the tracks and the starting points of cell movement, respectively. Error bars represent the standard deviations for 20 cells (d).

involved in breast cancer cell migration, we carried out *in vitro* migration assays using MDA-MB-231 and MDA-MB-435S cells treated with the membrane-permeable zinc chelator TPEN. In *in vitro* migration assays, TPEN inhibited the migration of MDA-MB-231 cells (Fig. 4b,c,d). This inhibition was neutralized by the addition of free zinc ion in the culture medium (Fig. 4b), indicating that the effect of TPEN was simply due to its chelation activity, not due to the other toxicities of the reagent. The chelation of intracellular Cu, Fe and Mn by 10 μM disodium bathocuproine disulfonate, 10 μM 2,2'-dipyridyl and 10 μM sodium para-aminosalicylic acid, respectively, did not inhibit migratory activity of MDA-MB-231 cells (Fig. 4b). Similar results were obtained using the MDA-MB-435S cells (Fig. 4a,c,d). Thus, intracellular zinc has essential functions in the migratory activity of these breast cancer cells. In addition, the defect in the migratory activity of the ZIP10-knockdown MDA-MB-231 and MDA-MB-435S cells could not be rescued by raising the level of intracellular free zinc ion using $ZnCl_2$ with or without zinc ionophore pyrithione (Fig. 4a), suggesting that zinc transported by ZIP10, but not intracellular free zinc ion, was necessary for breast cancer cell migration. Together, these results indicate that the zinc transporter ZIP10 is significantly involved in the migratory activity of MDA-MB-231 and MDA-MB-435S cells, and that the zinc transported via ZIP10 has essential functions in the migratory behavior of these breast cancer cells.

Discussion

Previous studies have indicated that zinc is related to the progression of cancers,[18] including carcinoma of the prostate[4] and liver.[7] The involvement of some kinds of zinc transporters in cancer metastasis, such as the lymph node metastasis of breast cancers, has also been reported.[15]

Our experiments established that zinc transported via ZIP10 but not ZIP6 is involved in the invasive behavior of breast cancer cells. Four lines of evidence support this idea. First, the depletion of intracellular zinc and ZIP10 in invasive breast cancer cells caused similar defects in the migratory activity of these cells. Second, the knockdown of ZIP10 in invasive breast cancer cells caused the downregulation of their zinc-uptake activity. Third, the expression level of *ZIP10* mRNA in breast cancer

cell lines was correlated with their invasiveness. Finally, the expression of *ZIP10* mRNA in clinical breast tumor samples was correlated with metastasis to lymph nodes.

Many previous reports have shown that zinc levels are higher in breast cancer than in normal breast tissue,[6,8,9,19] and that breast cancer tissue has a significantly high uptake of zinc.[20] In contrast, the serum zinc level is lower in patients with advanced breast cancers, leading to the idea that measuring the serum zinc levels could be useful for estimating the extent and prognosis of malignant breast diseases.[3,21,22] In our study, highly metastatic and advanced breast cancers showed higher expression of the ZIP10 zinc transporter than non-metastatic breast cancers. ZIP10 functions as a zinc importer, so our data suggest that more advanced breast cancers, which express high levels of ZIP10, can import larger amounts of zinc into the cytosol from the serum. This is consistent with previous observations of a high zinc level in advanced breast cancer tissue and a corresponding low level in serum. It is possible that highly metastatic and advanced breast cancers take in more zinc at least in part via the ZIP10 transporter, thereby acquiring greater migratory activities.

Our experiments showed that impaired migratory activity by ZIP10 suppression was not recoverable by increasing the intracellular free zinc ion level. This indicates that not free zinc ion but only the zinc transported via ZIP10 is essential for the increased migratory activity of breast cancer cells. Considering that intracellular free zinc ion is quite a little and almost all intracellular zinc exists in a form bound to zinc-containing molecules, our results suggest that there might be a specific chaperon molecule that transfers zinc imported through each zinc transporter to its functional target molecule, which requires zinc to regulate cell migration activities. This might be one of the mechanisms underlying the functional difference between ZIP10 and ZIP6 in cancer migratory activity.

Our study demonstrated an involvement of ZIP10 in human breast cancer progression and invasion. However, previous reports have shown that the ZIP6–LIV1 zinc transporter is involved in breast cancer metastasis to the lymph node.[15] ZIP10 and ZIP6 are most closely related to each other in the ZIP zinc transporter family, based on amino acid sequence,[23] indicating that they may have similar functions in regulating cell migration. However, our present study clearly showed that ZIP6 has no significant role in zinc uptake and cell migration of breast cancer cells, even though the basal expression level of ZIP6 is much higher than that of ZIP10. In addition, our clinicopathological analysis also indicated that high ZIP6 mRNA expression is associated with better prognostic parameters, which is consistent with a recent report about ZIP6.[16] Thus we think that ZIP10, but not ZIP6, plays a major role in breast cancer progression. At the moment, we do not know the reason why there is a functional difference between ZIP10 and ZIP6. This issue remains to be clarified.

Our present data showed that *ZIP10* expression had close correlations with epithelial–mesenchymal transition (EMT) markers such as E-cadherin and vimentin, whereas *ZIP6* expression did not. This suggested the involvement of ZIP10 in EMT, but the suppression of ZIP10 changed neither the morphologies nor the EMT markers of MDA-MB-231 or MDA-MB-435S cells (data not shown). Although we previously reported the involvement of zinc transporter ZIP6 in EMT during gastrulation of zebrafish,[24] the similar involvement of zinc transporter ZIP10 in EMT of human breast cancer was not shown, at least in the two breast cancer cell lines we examined. This may be due to the difference between normal cells and cancer cells. Furthermore, this suggested that ZIP10 regulates cancer cell migratory activities by other mechanisms. To clarify this issue, we investigated the expression of cell adhesion molecules, but we found no significant effects of ZIP10 knockdown on the levels of extracellular matrix proteins such as fibronectin and vitronectin, their receptors, including integrin family members α1–5, V, and β1, 3 and 5, or integrin-binding proteins, such as β-catenin, vinculin and talin (data not shown). In the meantime, zinc involvement in cytoskeleton-dependent cellular phenomena have been described, in the Fc-epsilon receptor I (RI)-induced translocation of granules in mast cell degranulation,[25] and the lipopolysaccharide (LPS)-induced upregulation of major histocompatibility complex class II and costimulatory molecules in dendritic cells.[26] These studies support our idea that zinc is probably involved in the cytoskeletal reorganization of breast cancer cells, although this issue remains to be clarified. Further investigations are needed to elucidate the novel mechanisms behind zinc- and ZIP10-dependent cancer cell migration.

Two recent reports demonstrate the zinc-uptake activity of ZIP10 and its metal-regulatory transcription factor 1 (MTF-1)-dependent expression; however, neither report refers to the biological functions of ZIP10.[17,27] The present study is the first to demonstrate a role for zinc and ZIP10 in cancer development, although the elucidation of the precise molecular mechanisms of their involvement will require further study. Our data suggest that ZIP10 may be a candidate marker for the metastatic phenotype of breast cancer and a promising target of novel treatment strategies, in addition to providing a new conceptual basis for understanding zinc-dependent signaling.

Acknowledgments

We thank S. Yamashita for his critical comments and helpful suggestions. We thank R. Masuda for secretarial assistance. This work was supported by grants from the Ministry of Education, Culture, Sports, Science and Technology in Japan, and the Japan Society for the Promotion of Science Research Fellowship Division.

References

1 Vallee BL, Falchuk KH. The biochemical basis of zinc physiology. *Physiol Rev* 1993; **73**: 79–118.
2 Vallee BL, Auld DS. Zinc coordination, function, and structure of zinc enzymes and other proteins. *Biochemistry* 1990; **29**: 5647–59.
3 Chakravarty PK, Ghosh A, Chowdhury JR. Zinc in human malignancies. *Neoplasma* 1986; **33**: 85–90.
4 Costello LC, Franklin RB. The clinical relevance of the metabolism of prostate cancer; zinc and tumor suppression: connecting the dots. *Mol Cancer* 2006; **5**: 17.
5 Gupta SK, Singh SP, Shukla VK. Copper, zinc, and Cu/Zn ratio in carcinoma of the gallbladder. *J Surg Oncol* 2005; **91**: 204–8.
6 Margalioth EJ, Schenker JG, Chevion M. Copper and zinc levels in normal and malignant tissues. *Cancer* 1983; **52**: 868–72.
7 Tashiro H, Kawamoto T, Okubo T, Koide O. Variation in the distribution of trace elements in hepatoma. *Biol Trace Elem Res* 2003; **95**: 49–63.
8 Schwartz AE, Leddicotte GW, Fink RW, Friedman EW. Trace elements in normal and malignant human breast tissue. *Surgery* 1974; **76**: 325–9.
9 Mulay IL, Roy R, Knox BE, Suhr NH, Delaney WE. Trace-metal analysis of cancerous and noncancerous human tissues. *J Natl Cancer Inst* 1971; **47**: 1–13.
10 Eide DJ. The SLC39 family of metal ion transporters. *Pflugers Arch* 2004; **447**: 796–800.
11 Gaither LA, Eide DJ. Eukaryotic zinc transporters and their regulation. *Biometals* 2001; **14**: 251–70.
12 Liuzzi JP, Cousins RJ. Mammalian zinc transporters. *Annu Rev Nutr* 2004; **24**: 151–72.
13 Palmiter RD, Huang L. Efflux and compartmentalization of zinc by members of the SLC30 family of solute carriers. *Pflugers Arch* 2004; **447**: 744–51.
14 Franklin RB, Feng P, Milon B *et al.* hZIP1 zinc uptake transporter down regulation and zinc depletion in prostate cancer. *Mol Cancer* 2005; **4**: 32.
15 Manning DL, Robertson JF, Ellis IO *et al.* Oestrogen-regulated genes in breast cancer: association of pLIV1 with lymph node involvement. *Eur J Cancer* 1994; **30A**: 675–8.
16 Kasper G, Weiser AA, Rump A *et al.* Expression levels of the putative zinc

doi: 10.1111/j.1349-7006.2007.00446.x

transporter LIV-1 are associated with a better outcome of breast cancer patients. *Int J Cancer* 2005; **117**: 961–73.
17 Kaler P, Prasad R. Molecular cloning and functional characterization of novel zinc transporter, rZip10 (Slc39a10), involved in zinc uptake across rat renal brush border membrane. *Am J Physiol Renal Physiol* 2007; **292**: F217–29.
18 Prasad AS, Kucuk O. Zinc in cancer prevention. *Cancer Metastasis Rev* 2002; **21**: 291–5.
19 Rizk SL, Sky-Peck HH. Comparison between concentrations of trace elements in normal and neoplastic human breast tissue. *Cancer Res* 1984; **44**: 5390–4.
20 Tupper R, Watts RW, Wormall A. The incorporation of ^{65}Zn in mammary tumours and some other tissues of mice after injection of the isotope. *Biochem J* 1955; **59**: 264–8.
21 Gupta SK, Shukla VK, Vaidya MP *et al.* Serum trace elements and Cu/Zn ratio in breast cancer patients. *J Surg Oncol* 1991; **46**: 178–81.
22 Yucel I, Arpaci F, Ozet A *et al.* Serum copper and zinc levels and copper/zinc ratio in patients with breast cancer. *Biol Trace Elem Res* 1994; **40**: 31–8.
23 Kambe T, Yamaguchi-Iwai Y, Sasaki R, Nagao M. Overview of mammalian zinc transporters. *Cell Mol Life Sci* 2004; **61**: 49–68.
24 Yamashita S, Miyagi C, Fukada T, Kagara N, Che YS, Hirano T. Zinc transporter LIVI controls epithelial–mesenchymal transition in zebrafish gastrula organizer. *Nature* 2004; **429**: 298–302.
25 Kabu K, Yamasaki S, Kamimura D *et al.* Zinc is required for Fc epsilon RI-mediated mast cell activation. *J Immunol* 2006; **177**: 1296–305.
26 Kitamura H, Morikawa H, Kamon H *et al.* Toll-like receptor-mediated regulation of zinc homeostasis influences dendritic cell function. *Nat Immunol* 2006; **7**: 971–7.
27 Wimmer U, Wang Y, Georgiev O, Schaffner W. Two major branches of anti-cadmium defense in the mouse: MTF-1/metallothioneins and glutathione. *Nucl Acids Res* 2005; **33**: 5715–27.

Clinicopathologic Analysis of Breast Cancers with *PIK3CA* Mutations in Japanese Women

Naomi Maruyama,[1,2] Yasuo Miyoshi,[1] Tetsuya Taguchi,[1] Yasuhiro Tamaki,[1] Morito Monden,[2] and Shinzaburo Noguchi[1]

Abstract

Purpose: Somatic mutations of *PIK3CA*, which encodes the p110α catalytic subunit of phosphatidylinositol 3-kinase, have recently been shown to play an important role in the pathogenesis and progression of human breast cancers. In this study, the frequency of *PIK3CA* mutations and their relationship with clinicopathologic and biological variables were investigated in Japanese breast cancers.

Experimental Design: Mutational analysis of *PIK3CA* was done in 188 primary breast cancers of Japanese women. Relationship of these mutations with various clinicopathologic variables [histologic type, tumor size, histologic grade, lymph node status, estrogen receptor (ER)-α and progesterone receptor status, and prognosis], biological variables [phospho-AKT (pAKT) and HER2 expression determined by immunohistochemistry], and *p53* mutation status was studied.

Results: Missense mutations of *PIK3CA* were found in 44 of 158 invasive ductal carcinomas, 4 of 10 invasive lobular carcinomas, 1 of 4 mucinous carcinomas, 2 of 2 squamous carcinomas, and 2 of 2 apocrine carcinomas, but no mutation was found in 12 noninvasive ductal carcinomas. *PIK3CA*-mutated tumors were found to be more likely to be ER-α positive ($P < 0.05$) and pAKT positive ($P < 0.05$). There was no significant association between *PIK3CA* mutations and *p53* mutation status. *PIK3CA* mutations were significantly ($P < 0.05$) associated with a favorable prognosis, and multivariate analysis showed that *PIK3CA* mutation status was a significant ($P < 0.05$) prognostic factor independent of the other conventional prognostic factors.

Conclusions: The frequency of *PIK3CA* mutations in Japanese breast cancers is similar to that of Caucasian breast cancers. Association of *PIK3CA* mutations with positive pAKT and positive ER-α suggests that *PIK3CA* mutations might exert their effects through activation of the phosphatidylinositol 3-kinase/AKT/ER-α pathway. *PIK3CA* mutations seem to have a potential to be used as an indicator of favorable prognosis.

Phosphatidylinositol 3-kinase (PI3K) is an activator of AKT, which regulates many cellular processes implicated in tumorigenesis such as cell growth, cell survival, and cell migration (1–3). Actually, AKT has been shown to be frequently activated in various types of human tumors including breast cancers (4, 5), suggesting that the PI3K/AKT pathway plays an important role in the pathogenesis and progression of human breast cancers.

PI3K consists of heterodimers with catalytic subunits (p110α, p110β, or p110δ) and regulatory subunits (p85α, p85β, or p55δ; ref. 6). The catalytic subunits are composed of several modular domains: catalytic lipid kinase domain, helical domain, C2 domain, Ras-binding domain, and the NH_2-terminal domain that interacts with the regulatory subunits. It is well established that PI3K is activated by autocrine or paracrine stimulation of receptor tyrosine kinases. Recently, in addition to this mechanism, somatic mutations of *PIK3CA*, which encodes the p110α catalytic subunit, have been shown to play an important role in the activation of PI3K in various human cancers (7–10). A high frequency of *PIK3CA* mutations has been reported in colorectal cancers, ovarian cancers, lung cancers, and breast cancers (7, 11–20). A great majority of somatic mutations in *PIK3CA* are missense mutations clustering in exons 9 and 20, which encode a part of the helical and kinase domains, respectively (7, 11, 13). *In vitro* studies have shown that the most frequently observed *PIK3CA* mutations in human breast cancers [i.e., E545K (exon 9) and H1047R (exon 20)] are associated with an increased kinase activity (8, 9), indicating that the *PIK3CA* mutations actually activate the PI3K pathway and thus are thought to be implicated in the pathogenesis and progression of breast cancers.

PIK3CA mutations, because they are found in 20% to 40% of breast cancers (11–14, 17), are considered to be one of the

Authors' Affiliations: Departments of [1]Breast and Endocrine Surgery and [2]Surgery and Clinical Oncology, Osaka University Graduate School of Medicine, Osaka, Japan

Received 2/6/06; revised 9/15/06; accepted 9/27/06.

Grant support: Grant-in-Aid for Cancer Research from the Ministry of Health, Labor and Welfare of Japan, for Scientific Research on Priority Areas from the Ministry of Education, Culture, Sports, Science and Technology of Japan, and for Scientific Research from the Japanese Breast Cancer Society.

The costs of publication of this article were defrayed in part by the payment of page charges. This article must therefore be hereby marked *advertisement* in accordance with 18 U.S.C. Section 1734 solely to indicate this fact.

Requests for reprints: Shinzaburo Noguchi, Department of Breast and Endocrine Surgery, Osaka University Graduate School of Medicine, 2-2 Yamadaoka, Suita-shi, Osaka 565-0871, Japan. Fax: 81-6-6879-3779; E-mail: noguchi@onsurg.med.osaka-u.ac.jp.

doi:10.1158/1078-0432.CCR-06-0267

most commonly observed genetic changes besides *p53* mutations and *HER2* amplification. Although many reports have been available on the clinicopathologic characteristics of breast cancers with *p53* mutations or *HER2* amplification (21, 22), only a few reports have been available thus far on the clinicopathologic characteristics of breast cancers with *PIK3CA* mutations (11, 23). Elucidation of the characteristics of breast cancers with *PIK3CA* mutations seems to be important for the execution of personalized medicine in future. In addition, all the studies reported until now on *PIK3CA* mutations dealt with Caucasian breast cancers. It seems to be interesting to compare the frequency of *PIK3CA* mutations between Japanese and Caucasian breast cancers because breast cancer incidence in Japanese women is much lower (one fourth) than that of Caucasian women and, thus, contribution of *PIK3CA* mutations to pathogenesis of breast cancers might be different between two ethnicities. Therefore, in the present study, we have analyzed somatic mutations of *PIK3CA* in Japanese breast cancers as well as their relationship with the various clinicopathologic variables including patient prognosis. To further characterize breast cancers with *PIK3CA* mutations, correlation of *PIK3CA* mutations with phospho-AKT (pAKT) expression, HER2 overexpression, or *p53* mutation status has also been studied.

Materials and Methods

Patients and surgical specimens. Tumor tissue samples were obtained from 188 primary breast cancer patients who underwent mastectomy or breast conserving surgery during the period from March 1998 to October 2002 at Osaka University Hospital. Tumor tissue samples were obtained from the surgical specimens and snap frozen in liquid nitrogen and kept at −80°C until use. Informed consent was obtained from each patient before surgery.

As adjuvant chemotherapy (Table 1), six cycles of CMF (cyclophosphamide 100 mg/d orally days 1-14 + methotrexate 40 mg/m^2 i.v. days 1 and 8 + 5-fluorouracil 600 mg/m^2 i.v. days 1 and 8 q4w) were given to 15 patients, four cycles of EC (epirubicin 60 mg/m^2 i.v. day 1 + cyclophosphamide 600 mg/m^2 i.v. day 1 q3w) were given to 12 patients, and four cycles of docetaxel 60 mg/m^2 i.v. day 1 q3w were given to 4 patients. One hundred patients were treated with adjuvant hormonal therapy [tamoxifen 20 mg/d (n = 77), tamoxifen 20 mg/d + goserelin 3.6 mg q4w (n = 23)]. Forty-seven patients were treated with combination of chemotherapy [CMF (n = 21), EC (n = 21), or other chemotherapies (n = 5)] and hormonal therapy [tamoxifen (n = 44), goserelin (n = 1), or tamoxifen + goserelin (n = 2)]. Ten patients received no adjuvant therapy. Duration of tamoxifen treatment was 5 years and that of goserelin treatment was 2 years in most cases. Indication for adjuvant treatment was decided essentially according to the St. Gallen recommendation (24).

Physical examination every 3 months for 2 years postoperatively and every 6 months thereafter, combined with blood test and chest X-ray examination every 6 months postoperatively, was done. The median follow-up period of these 188 patients was 64 months, ranging from 38 to 88 months. Forty-five patients developed recurrences (i.e., 16 developed bone metastases, 9 developed liver metastases, 5 developed brain metastases, 6 developed lung metastases, 4 developed soft tissue metastases, and 12 developed lymph node metastases). Ipsilateral breast recurrences after breast conserving surgery were not counted as recurrences.

***Mutational analysis of* PIK3CA.** PCR amplification was done with the primers previously described for exons 1, 2, 4, 7, 9, 13, 18, and 20 of *PIK3CA* (7). Sequencing of the PCR products was done using an ABI 3300 automated capillary sequencer. We obtained the sequence data of *PIK3CA* gene from GenBank (accession no. NM_006218). Genomic DNA from corresponding normal tissue was subjected to sequence analysis to confirm that the nucleotide substitutions detected in tumor tissues are somatic in nature as for samples when nucleotide changes were detected in tumor tissues.

Immunohistochemistry of pAKT, HER2, and phospho-S6 expression. The expression of pAKT, HER2, and phospho-S6 (pS6) was studied by immunohistochemistry. In brief, for pAKT and pS6, endogeneous peroxidases were quenched by incubating the sections for 10 min in 6% H_2O_2. After several washes in TBS-T, antigen retrieval was done by heating the samples in 10 mmol/L citrate buffer (pH 6.0) at 95°C for 40 min. After blocking serum (DAKO Diagnostics, Mississauga, Ontario, Canada) for 30 min, the samples were incubated with a polyclonal rabbit anti-pAKT (Ser^{473}) antibody (1:100 dilution; Cell Signaling Technologies, Beverly, MA) or with a polyclonal anti-phospho-S6 ribosomal protein (1:50 dilution; Cell Signaling Technologies) at 4°C overnight. We then used the LSAB+ System (DAKO), which involved incubation with streptavidin treatment followed by secondary antibody for signal amplification (pAKT), or an avidin-biotin method (pS6). The positive reaction of pAKT was scored into four grades according to the intensity of the staining (0, none; 1+, weakly positive; 2+, moderately positive; and 3+, strongly positive) according to the method previously reported (25, 26). 0 and 1+ recorded as negative and 2+ and 3+ recorded as positive (Fig. 1). As for the cutoff level of pS6, we have scored both staining intensity and the percent of positive cells according to Allred scoring (27). The proportion score varies from 0 to 5 [0 (none or negative), 1 (<1/100), 2 (1/100-1/10), 3 (1/10-1/3), 4 (1/3-2/3), and 5 (>2/3)] and intensity score is the average intensity of all the positive cells (0, negative; 1, weak; 2, intermediate; and 3, strong). We classified positive when the total score that was obtained by summing proportion score and intensity score was >3. HER2 score was determined according to the DAKO system scale (DAKO Diagnostics, Vienna, Austria): HER2 negative (0 and 1+) and HER2 positive (2+ and 3+).

***Mutational analysis of* p53.** For identify genomic abnormalities of *p53*, each exon-intron junction from exon 5 to exon 8 was screened using PCR-single-strand conformation polymorphism method or direct sequencing, following the method previously described (28). Nucleotide alterations detected by single-strand conformation polymorphism were determined by sequencing analysis.

Estrogen receptor and progesterone receptor assay. Estrogen receptor (ER) and progesterone receptor (PR) contents of breast cancer tissues were measured by means of enzyme immunoassay using the kit provided by Abbott Research Laboratories (Chicago, IL). The cutoff value was 5 fmol/mg protein for ER and PR in accordance with the manufacturer's instruction.

Statistics. The relationship between *PIK3CA* mutation status and clinicopathologic variables of breast tumors was analyzed by the χ^2 test or Kruskal-Wallis test. Relapse-free survival curves were calculated by the Kaplan-Meier method, and the log-rank test was used to evaluate the differences in relapse-free survival rates. Cox proportional hazards model was used to calculate the hazard ratio for each variable in the univariate and multivariate analyses. Statistical significance was defined as $P < 0.05$.

Results

Frequency and location of* PIK3CA *mutations. Mutational analysis of *PIK3CA* was done in 188 primary breast cancers and, finally, 54 missense mutations were identified in total (Fig. 2). Because all the mutations were not detected in the corresponding normal tissues, these mutations were confirmed as somatic mutations. Of these 54 mutations, 17 and 29 mutations clustered in exon 9 and exon 20, respectively.

PIK3CA ***mutations and clinicopathologic characteristics of breast cancers.*** The frequency of *PIK3CA* mutations according

Table 1. Regimens used in postoperative adjuvant chemotherapy and/or hormonal therapy for breast cancer patients

	Mutation (+)	Mutation (−)	Total	P
Chemotherapy	6	25	31	
EC (4 cycles)*	3	9	12	
CMF (6 cycles)†	3	12	15	0.55
TXT (4 cycles)‡	0	4	4	
Hormonal therapy	31	69	100	
Tamoxifen§	24	53	77	0.99
Tamoxifen + goserelin‖	7	16	23	
Chemotherapy + hormonal therapy	16	31	47	
CMF (6 cycles) + tamoxifen	8	13	21	
EC (4 cycles) + tamoxifen	5	13	18	
TXT + tamoxifen	1	2	3	0.92
EC (4 cycles) + goserelin	0	1	1	
EC (4 cycles) + tamoxifen + goserelin	1	1	2	
Others + tamoxifen	1	1	2	
No therapy	1	9	10	

*Epirubicin 60 mg/m^2 i.v. day 1 + cyclophosphamide 600 mg/m^2 i.v. day 1 q3w.
†Cyclophosphamide 100 mg/d orally days 1-14 + methotrexate 40 mg/m^2 i.v. days 1 and 8 + 5-fluorouracil 600 mg/m^2 i.v. days 1 and 8 q4w.
‡Docetaxel 60 mg/m^2 i.v. day 1 q3w.
§Tamoxifen 20 mg/d.
‖Goserelin 3.6 mg q4w.

to histologic types is shown in Table 2. *PIK3CA* mutations were found in 44 of 158 (28%) invasive ductal carcinomas, 4 of 10 (40%) invasive lobular carcinomas, 1 of 4 (25%) mucinous carcinomas, 2 of 2 (100%) squamous carcinomas, and 2 of 2 (100%) apocrine carcinomas, but no mutation was found in 12 noninvasive ductal carcinomas.

The relationship of *PIK3CA* mutations with clinicopathologic variables is shown in Table 3. The frequency of *PIK3CA* mutations in ER-positive tumors (34%) was significantly ($P < 0.05$) higher than that in ER-negative tumors (19%), and the frequency of *PIK3CA* mutations in PR-positive tumors (33%) tended ($P = 0.09$) to be higher than that in PR-negative tumors (22%). *PIK3CA* mutation status was not significantly associated with menopausal status, tumor size, lymph node status, or histologic grade.

Relationship of* PIK3CA *mutations with pAKT or HER2 expression and* p53 *mutation status. Because it is suggested that *PIK3CA* mutations activate AKT function through its phosphorylation, we investigated the relationship between *PIK3CA* mutations and expression of pAKT. The frequency of *PIK3CA* mutations was significantly ($P < 0.05$) higher in pAKT-positive tumors (66%) than pAKT-negative tumors (40%; Table 4). We also studied the relationship between *PIK3CA* mutations and HER2 expression or *p53* mutations (Table 4). HER2 expression and *p53* mutations were not significantly associated with *PIK3CA* mutations.

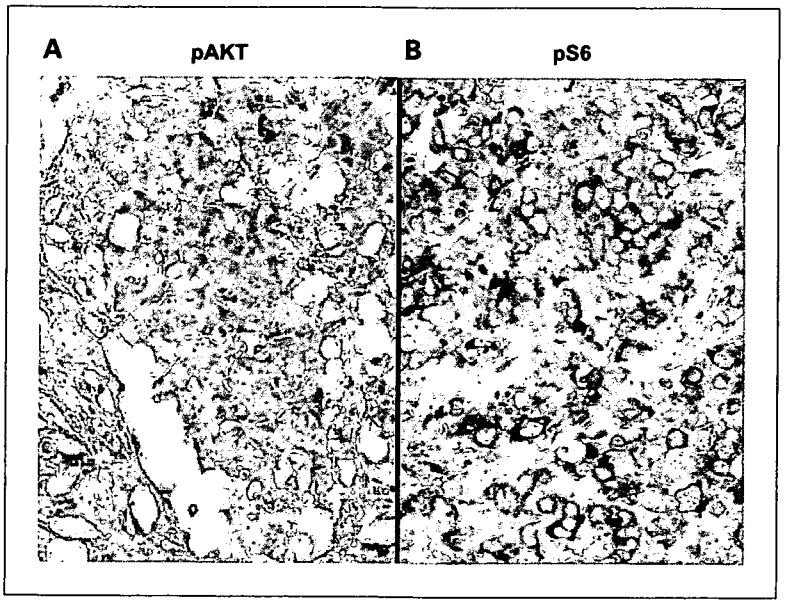

Fig. 1. Representative results of immunohistochemical staining of pAKT, pS6, and PTEN in breast cancer tissues. *A*, pAKT (×400); *B*, pS6 (×400).

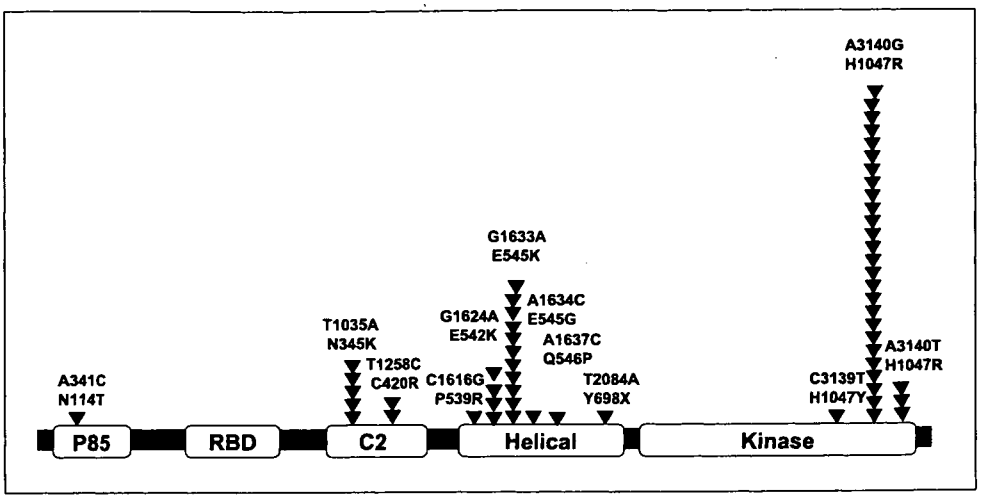

Fig. 2. Location of *PIK3CA* mutations in breast cancers. Arrowheads, location of missense mutations; boxes, functional domains.

Relationship of pAKT expression with pS6 expression. To further confirm the downstream activation of PI3K/AKT pathway induced by the *PIK3CA* mutations, we have investigated pS6, a downstream target molecule of pAKT by immunostaining. As shown in Table 5, the frequency of pS6-positive tumors was significantly ($P < 0.05$) higher in pAKT-positive tumors (76%) than in pAKT-negative tumors (51%).

PIK3CA *mutations and patient prognosis.* The relationship of *PIK3CA* mutations with patient prognosis was analyzed in 176 invasive carcinomas. The relapse-free survival rates of patients with *PIK3CA* mutations were significantly ($P < 0.05$) better than those of patients without them in the total patients (Fig. 3A) as well as in the subset of patients with ER-α-positive tumors (Fig. 3B). Univariate analysis showed that *PIK3CA* mutation status, tumor size, lymph node status, ER-α status, and PR status were significant ($P < 0.05$) prognostic factors, and multivariate analysis showed that *PIK3CA* mutation status, tumor size, lymph node status, and PR status were significant ($P < 0.05$) and mutually independent prognostic factors (Table 6).

Discussion

In the present study, we have identified *PIK3CA* mutations in 29% (54 of 188) of Japanese breast cancers including two novel missense mutations (N114T in exon 1 and Y698X in exon 13). Majority [83% (45 of 54)] of the mutations clustered in exon 9 and exon 20, helical and kinase domains, respectively. Not only the frequency but also the location of *PIK3CA* mutations is quite similar to that reported in Caucasian breast cancers (11). These results indicate that the contribution of *PIK3CA* mutations to pathogenesis and progression of breast cancers might be similar between two ethnicities.

No *PIK3CA* mutation was found in 12 noninvasive ductal carcinomas in the present study and Lee et al. reported *PIK3CA* mutations in only 2 of 15 (13%) noninvasive ductal carcinomas. These mutation frequencies in noninvasive ductal carcinomas seem to be slightly lower than those reported in invasive ductal carcinomas (20-40%). Because AKT stimulates tumor invasion by promoting the secretion of matrix metalloproteinases (29, 30) and the induction of epithelial-mesenchymal transition (31, 32), it is speculated that *PIK3CA* mutations

Table 2. *PIK3CA* mutations and histologic types of breast cancers

Histologic types	*PIK3CA* mutations (%)
Noninvasive ductal carcinoma	0 of 12 (0)
Invasive carcinoma	54 of 176 (31)
Invasive ductal carcinoma	44 of 158 (28)
Invasive lobular carcinoma	4 of 10 (40)
Mucinous carcinoma	1 of 4 (25)
Squamous cell carcinoma	2 of 2 (100)
Apocrine carcinoma	2 of 2 (100)

Table 3. *PIK3CA* mutations and clinicopathologic variables of breast cancers

	PIK3CA		*n*	*P*
	Mutant (%)	Wild (%)		
Menopausal status				
Premenopausal	29 (32)	63 (68)	92	
Postmenopausal	25 (26)	71 (74)	96	NS
Tumor size (cm)*				
>2	19 (31)	43 (69)	62	
≤2	35 (31)	79 (69)	114	NS
Lymph node metastasis*				
Negative	33 (31)	74 (69)	107	
Positive	21 (31)	46 (69)	67	NS
Unknown			2	
Histologic grade*				
1	9 (32)	19 (68)	28	
2	37 (33)	74 (67)	111	NS
3	3 (14)	19 (86)	22	
Unknown			15	
ER				
Positive	42 (34)	82 (66)	124	
Negative	12 (19)	52 (81)	64	0.03
PR				
Positive	38 (33)	76 (67)	114	
Negative	16 (22)	57 (78)	73	0.09
Unknown			1	

Abbreviation: NS, not significant.
*Noninvasive ductal carcinomas were excluded.

Table 4. Relationship between *PIK3CA* mutations and pAKT, HER2 expression, and *p53* mutations

	PIK3CA		*n*	*P*
	Mutant (%)	Wild (%)		
pAKT				
Positive	19 (66)	10 (34)	29	0.03
Negative	19 (40)	28 (60)	47	
HER2				
Positive	9 (38)	15 (62)	24	NS
Negative	39 (33)	80 (67)	119	
p53				
Mutant	9 (27)	24 (73)	33	NS
Wild	45 (29)	110 (71)	155	

might play a certain role in the progression from noninvasive to invasive ductal carcinomas through the activation of AKT.

The frequency of *PIK3CA* mutations in breast cancers with histologic types other than ductal carcinomas has rarely been reported (13). Although the number of tumors with histologic types other than invasive ductal carcinomas is small in the present study, we have been able to show that *PIK3CA* mutations are found in 4 of 10 invasive lobular carcinomas, 1 of 4 mucinous carcinomas, 2 of 2 squamous carcinomas, and 2 of 2 apocrine carcinomas. These results indicate that *PIK3CA* mutations are implicated in the pathogenesis and progression of not only ductal carcinomas but also other types of breast cancers. Recently, Buttitta et al. (33) have reported that the frequency of *PIK3CA* mutations is higher in invasive lobular carcinomas than in invasive ductal carcinomas, being consistent with our present observation that the frequency of *PIK3CA* mutations was 40% in invasive lobular carcinomas and 28% in invasive ductal carcinomas. One characteristic phenotype of invasive lobular carcinomas is its high ER positivity (34, 35). This phenotype of invasive lobular carcinomas seems to be explained, at least in part, by the higher frequency of *PIK3CA* mutations, which are associated with ER-α-positive breast cancers.

It has been reported that the hotspot mutations in *PIK3CA* actually enhance the lipid kinase activity as compared with wild type, leading to the increased phosphorylation of AKT and the resultant transformation of normal breast epithelial cells to tumor cells by *in vitro* and *in vivo* studies (8, 9). To examine whether the *PIK3CA* mutations found in the present study actually activate AKT through phosphorylation in human breast cancers, immunohistochemical study using anti-pAKT specific antibody was done. As expected, the frequency of *PIK3CA* mutations was significantly ($P < 0.05$) higher in pAKT-positive tumors (66%) than in pAKT-negative tumors (40%), suggesting that activation of AKT through phosphorylation by *PIK3CA* mutations actually occurs in human breast cancers. Furthermore, to confirm whether the pAKT activates downstream targets, the relationship between pAKT and phosphorylation of S6, one of the target molecules phosphorylated by pAKT signaling, was investigated by immunostaining. The positive correlation between pAKT and pS6 might suggest a downstream activation of this signal transduction induced by *PIK3CA* mutations.

The PI3K/AKT pathway regulates the various important cell functions implicated in tumorigenesis including cell growth, cell survival, and cell migration. In the present study, we have found that *PIK3CA* mutations are significantly higher in ER-α-positive tumors than in ER-α-negative tumors. Saal et al. (11) also reported a significant association between *PIK3CA* mutations and ER-α tumors. A positive association between pAKT and ER-α was also shown by an immunohistochemical study in breast cancers (36). Recently, it has been shown that AKT phosphorylates Ser^{167} of ER-α and enhances the transcriptional activity of ER-α (37). Thus, it is speculated that, in tumor cells with *PIK3CA* mutations, the PI3K/AKT/ER-α pathway might be activated, resulting in the preferential growth of ER-α-positive tumors.

Because the effect of *PIK3CA* mutations on patient prognosis has rarely been studied, we have investigated the prognostic significance of *PIK3CA* mutations in the present study. *PIK3CA* mutations activate AKT through phosphorylation and the pAKT expression has been reported to be associated with poor prognosis (38). The reason for such an association is considered to be attributable to resistance of pAKT-positive tumors to adjuvant tamoxifen, being based on the findings that prognosis of pAKT-positive tumors is poorer than that of pAKT-negative tumors in the ER-α-positive group treated with adjuvant tamoxifen but not in that treated without adjuvant tamoxifen. Thus, we assumed that tumors with *PIK3CA* mutations would be associated with poor prognosis in the present study where almost all patients (93%) with ER-α-positive tumors had been treated with tamoxifen. Until now, only two reports have been available on the relationship between *PIK3CA* mutations and prognosis. Li et al. (23) reported a significant association of *PIK3CA* mutations with poor prognosis, but Saal et al. (11) failed to confirm such an association. In the present study, we have obtained an unexpected result that tumors with *PIK3CA* mutations are significantly associated with a favorable prognosis in the total patients as well as in the subset of patients with ER-α-positive tumors.

Our result that *PIK3CA* mutations are associated with a favorable prognosis seems to be inconsistent with the fact that pAKT-positive tumors are associated with poor prognosis (38). In *PIK3CA*-mutated tumors, the PI3K/AKT pathway is probably the principal pathway for carcinogenesis and progression. However, in pAKT-positive tumors, because AKT is activated not only by *PIK3CA* mutations but also by various growth factors, other pathways (e.g., extracellular signal–regulated kinase/mitogen-activated protein kinase pathway) are very likely to be activated in addition to the PI3K/AKT pathway. Therefore, it is not surprising that the biological behaviors of the *PIK3CA*-mutated tumors and pAKT-positive tumors are different. Very recently, it has been shown that breast cancer cells with *PIK3CA* mutations are more likely to respond to tamoxifen than those without them as opposed to the findings that pAKT is associated with a resistance to

Table 5. Relationship between pAKT expression and pS6 expression

	pS6		*n*	*P*
	Positive (%)	Negative (%)		
pAKT				
Positive	22 (76)	7 (24)	29	0.03
Negative	24 (51)	23 (49)	47	

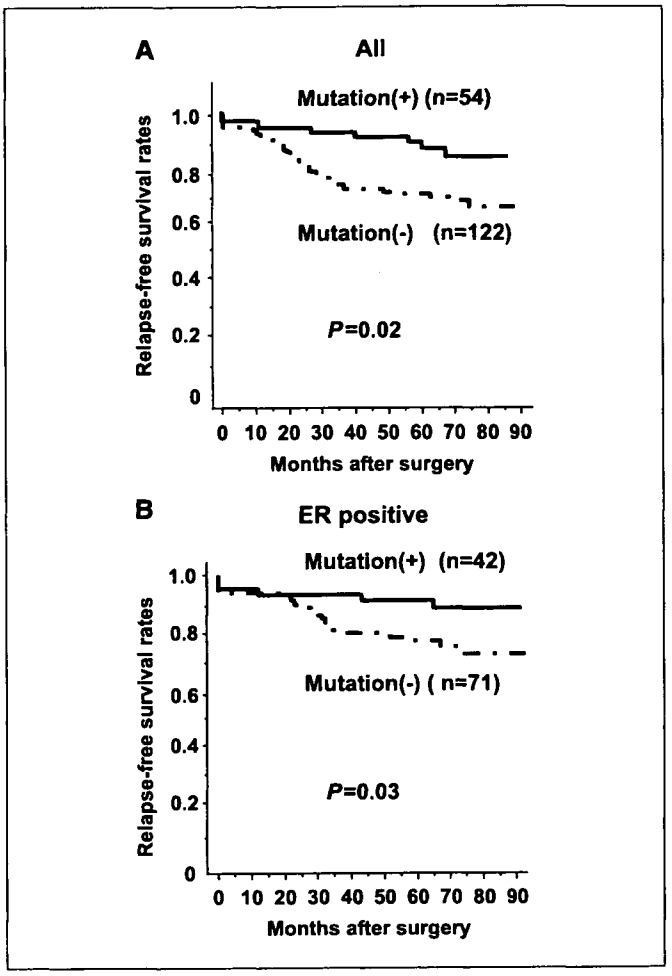

Fig. 3. Relapse-free survival rates of total patients with breast cancers (*A*) and patients with ER-α-positive breast cancers (*B*).

tamoxifen (39). We speculate that growth of tumor cells with *PIK3CA* mutations is highly dependent on estrogens due to the activation of the PI3K/AKT/ER-α pathway, and such cells are more likely to be growth inhibited by tamoxifen, and thus that *PIK3CA*-mutated tumors are associated with a favorable prognosis in patients treated with tamoxifen. Interestingly, recently, Yamashita et al. (37) have reported that phosphorylation of Ser^{167}, which is induced by pAKT, is associated with a good response to hormonal therapy including tamoxifen. Ideally, the effect of *PIK3CA* mutations on prognosis would better be analyzed in ER-positive breast cancer patients treated separately with and without tamoxifen to clarify whether *PIK3CA* mutation status would serve as a prognostic factor or as a predictive factor for response to tamoxifen. However, because almost all ER-positive breast cancer patients had been treated with tamoxifen, such an analysis was unable to be done in the present study.

Because both *PIK3CA* mutations and loss of phosphatase and tensin homologue (PTEN) function are thought to activate PI3K pathway, it is speculated that *PIK3CA* mutations and loss of PTEN expression are mutually exclusive. Consistent with this speculation, Saal et al. (11) have reported a negative association between *PIK3CA* mutations and loss of PTEN expression. Singh et al. (40) reported that *PIK3CA* mutations and *p53* mutations were mutually exclusive. Inconsistent with their report, however, we have found no association between *p53* mutations and *PIK3CA* mutations. The reason for these discrepancies is currently unknown; the relatively small number of tumors analyzed in these reports and the present study prevents from drawing a conclusion about the correlation of *PIK3CA* mutations with PTEN expression or *p53* mutations, and seems to indicate a necessity of further studies.

Because HER2 overexpression activates the PI3K/AKT pathway, tumors with *HER2* amplification are speculated not to require a further activation of this pathway by *PIK3CA* mutations. However, Saal et al. (11) reported a significant positive association between HER2 overexpression and *PIK3CA* mutations, suggesting that more than one input activating the PI3K/AKT pathway might be necessary for carcinogenesis of breast cancer. In the present study, we have failed to show a significant association between HER2 overexpression and *PIK3CA* mutations. Because immunohistochemistry is not an accurate method for determination of *HER2* amplification and only a limited number of breast cancers were analyzed in HER2 overexpression, our result needs to be interpreted with caution and should be confirmed by fluorescence *in situ* hybridization analysis of *HER2* amplification using a larger number of tumors.

In conclusion, we have identified somatic missense mutations of *PIK3CA* in 54 of 188 (29%) Japanese breast cancers. Majority (83%) of the mutations clustered in exon 9 and exon 20, helical and kinase domains, respectively. *PIK3CA* mutations were significantly associated with ER-α-positive tumors, or pAKT-positive tumors. Patients with *PIK3CA*-mutated tumors showed a significantly more favorable prognosis than those with *PIK3CA*-nonmutated tumors. It is currently unknown whether *PIK3CA* mutation status serves as a prognostic factor or as a predictive factor of response to tamoxifen. Our preliminary results need to be confirmed by a future study including a larger number of patients with a longer follow-up period.

Table 6. Univariate and multivariate analyses of various prognostic factors

	Univariate		Multivariate	
	HR* (95% CI)	P	HR* (95% CI)	P
PIK3CA mutation	2.36 (1.10-5.06)	0.03	2.34 (1.08-5.08)	0.03
Tumor size (cm)	6.25 (2.33-16.7)	0.0004	4.35 (1.54-12.5)	0.006
Lymph node status	3.03 (1.69-5.56)	0.0002	2.17 (1.18-4.17)	0.01
Histologic grade	1.27 (0.53-3.03)	0.59		
ER status	2.01 (1.13-3.59)	0.02	0.71 (0.33-1.53)	0.38
PR status	2.94 (1.61-5.35)	0.0004	2.96 (1.35-6.50)	0.007

NOTE: Noninvasive ductal carcinomas were excluded.
Abbreviation: CI, confidence interval.
*Hazard ratio of mutation negative against positive, large tumor (2.0 cm <) against small tumor (≤2.0 cm), lymph node positive against negative, histologic grade 2 + 3 against grade 1, ER-negative against ER-positive, and PR-negative against PR-positive.

References

1. Osaki M, Oshimura M, Ito H. PI3K-AKT pathway: its functions and alterations in human cancer. Apoptosis 2004;9:667–76.
2. Fresno Vara JA, Casado E, de Castro J, Cejas P, Belda-Iniesta C, Gonzalez-Baron M. PI3K/Akt signaling pathway and cancer. Cancer Treat Rev 2004;30: 193–204.
3. Stephens L, Williams R, Hawkins P. Phosphoinositide 3-kinases as drug targets in cancer. Curr Opin Pharmacol 2005;5:357–65.
4. Bellacosa A, de Feo D, Godwin AK, et al. Molecular alterations of the AKT2 oncogene in ovarian and breast carcinomas. Int J Cancer 1995;64:280–5.
5. Cheng JQ, Ruggeri B, Klein WM, et al. Amplication of AKT2 in human pancreatic cells and inhibition of AKT2 expression and tumorigenicity by antisense RNA. Prc Natl Acad Sci U S A 1996;93:3636–41.
6. Vanhaesebroeck B, Waterfield MD. Signaling by distinct classes of phosphoinositide 3-kinases. Exp Cell Res 1999;253:239–54.
7. Samuels Y, Wang Z, Bardelli A, et al. High frequency of mutations of the *PIK3CA* gene in human cancers. Science 2004;304:554.
8. Ikenoue T, Kanai F, Hikiba Y, et al. Functional analysis of *PIK3CA* gene mutations in human colorectal cancer. Cancer Res 2005;65:4562–7.
9. Samuels Y, Diaz LA, Jr., Schmidt-Kittler O, et al. Mutant *PIK3CA* promotes cell growth and invasion of human cancer cells. Cancer Cell 2005;7:561–73.
10. Kang S, Bader AG, Vogt PK. Phosphatidylinositol 3-kinase mutations identified in human cancer are oncogenic. Proc Natl Acad Sci U S A 2005;102:802–7.
11. Saal LH, Holm K, Maurer M, et al. *PIK3CA* Mutations correlate with hormone receptors, node metastasis, and ERBB2, and are mutually exclusive with PTEN loss in human breast carcinoma. Cancer Res 2005; 65:2554–9.
12. Levine DA, Bogomolniy F, Yee CJ, et al. Frequent mutation of the *PIK3CA* gene in ovarian and breast cancers. Clin Cancer Res 2005;11:2875–8.
13. Campbell IG, Russell SE, Choong DY, et al. Mutation of the *PIK3CA* gene in ovarian and breast cancer. Cancer Res 2004;64:7678–81.
14. Bachman KE, Argani P, Samuels Y, et al. The *PIK3CA* gene is mutated with high frequency in human breast cancers. Cancer Biol Ther 2004;3:772–5.
15. Broderick DK, Di C, Parrett TJ, et al. Mutations of *PIK3CA* in anaplastic oligodendrogliomas, high-grade astrocytomas, and medulloblastomas. Cancer Res 2005;64:5048–50.
16. Wang Y, Helland A, Holm R, Kristensen GB, Borresen-Dale AL. *PIK3CA* mutations in advanced ovarian carcinomas. Hum Mutat 2005;25:322.
17. Lee JW, Soung YH, Kim SY, et al. *PIK3CA* gene is frequency mutated in breast carcinomas and hepatocellular carcinomas. Oncogene 2005;24:1477–80.
18. Velho S, Oliveira C, Ferreira A, et al. The prevalence of *PIK3CA* mutations in gastric and colon cancer. Eur J Cancer 2005;41:1649–54.
19. Li VSW, Wong CW, Chan TL, et al. Mutaitons of *PIK3CA* in gastric adenocarcinoma. BMC Cancer 2005;5:29.
20. Wu G, Xing M, Mambo E, et al. Somatic mutation and gain of copy number of *PIK3CA* in human breast cancer. Breast Cancer Res 2005;7:609–16.
21. Slamon DJ, Clark GM, Wong SG, Levin WJ, Ullrich A, McGuire WL. Human breast cancer: correlation of relapse and survival with amplification of the *HER-2/neu* oncogene. Science 1987;235:177–82.
22. Kourea HP, Koutras AK, Scopa CD, et al. Expression of the cell cycle regulatory proteins p34cdc2, p21waf1, and p53 in node negative invasive ductal breast carcinoma. Mol Pathol 2003;56:328–35.
23. Li SY, Rong M, Grieu F, Iacopetta B. *PIK3CA* mutations in breast cancer are associated with poor outcome. Breast Cancer Res Treat 2006;96:91–5.
24. Goldhirsch A, Glick JH, Gelber RD, Coates AS, Thurlimann B, Senn HJ; Panel Members. Meeting highlights: International Expert Consensus on the Primary Therapy of Early Breast Cancer 2005. Ann Oncol 2005;16:1569–83.
25. Kucab JE, Lee C, Chen CS, et al. Celecoxib analogues disrupt Akt signaling, which is commonly activated in primary breast tumours. Breast Cancer Res 2005;7:796–807.
26. David O, Jett J, LeBeau H, et al. Phospho-Akt overexpression in non-small cell lung cancer confers significant stage-independent survival disadvantage. Clin Cancer Res 2004;10:6865–71.
27. Harvey JM, Clark GM, Osborne CK, Allred DC. Estrogen receptor status by immunohistochemistry is superior to the ligand-binding assay for predicting response to adjuvant endocrine therapy in breast cancer. J Clin Oncol 1999;17:1474–81.
28. Miyoshi Y, Iwao K, Takahashi Y, Egawa C, Noguchi S. Acceleration of chromosomal instability by loss of BRCA1 expression and p53 abnormality in sporadic breast cancers. Cancer Lett 2000;159:211–6.
29. Park BK, Zeng X, Glazer RI. Akt1 induces extracellular matrix invasion and matrix metalloproteinase-2 activity in mouse mammary epithelial cells. Cancer Res 2001;61:7647–53.
30. Thant AA, Nawa A, Kikkawa F, et al. Fibronectin activates matrix metalloproteinase-9 secretion via the MEK1-MAPK and the PI3K-Akt pathways in ovarian cancer cells. Clin Exp Metastasis 2000;18: 423–8.
31. Larue L, Bellacosa A. Epithelial-mesenchymal transition in development and cancer: role of phosphatidylinositol 3 kinase/AKT pathways. Oncogene 2005; 24:7443–54.
32. Grille SJ, Bellacosa A, Upson J, et al. The protein kinase Akt induces epithelial mesenchymal transition and promotes enhanced motility and invasiveness of squamous cell carcinoma lines. Cancer Res 2003;63: 2172–8.
33. Buttitta F, Felicioni L, Barassi F, et al. *PIK3CA* mutation and histological type in breast carcinoma: high frequency of mutations in lobular carcinoma. J Pathol 2006;208:350–5.
34. Middleton LP, Palacios DM, Bryant BR, Krebs P, Otis CN, Merino MJ. Pleomorphic lobular carcinoma: morphology, immunohistochemistry, and molecular analysis. Am J Surg Pathol 2000;24:1650–6.
35. Frolik D, Caduff R, Varga Z. Pleomorphic lobular carcinoma of the breast: its cell kinetics, expression of oncogenes, and tumor suppressor genes compared with invasive ductal carcinomas and classical infiltrating lobular carcinomas. Histopathology 2001;39: 503–13.
36. Kirkegaard T, Witton CJ, McGlynn LM, et al. AKT activation predicts outcome in breast cancer patients treated with tamoxifen. J Pathol 2005;207: 139–46.
37. Yamashita H, Nishio M, Kobayashi S, et al. Phosphorylation of estrogen receptor α serine 167 is predictive of response to endocrine therapy and increases postrelapse survival in metastatic breast cancer. Breast Cancer Res 2005;7:753–64.
38. Tokunaga E, Kimura Y, Oki E, et al. Akt is frequently activated in HER2/neu-positive breast cancers and associated with poor prognosis among hormone-treated patients. Int J Cancer 2006;118:284–9.
39. Whyte DB, Holbeck SL. Correlation of *PIK3CA* mutations with gene expression and drug sensitivity in NCI-60 cell lines. Biochem Biophys Res Commun 2006;340:469–75.
40. Singh B, Reddy PG, Goberdhan A, et al. p53 regulates cell survival by inhibiting PIK3CA in squamous cell carcinomas. Genes Dev 2002;16:984–93.

Breast Cancer Res Treat (2007) 101:305–315
DOI 10.1007/s10549-006-9293-x

EPIDEMIOLOGY

Possible involvement of CCT5, RGS3, and YKT6 genes up-regulated in p53-mutated tumors in resistance to docetaxel in human breast cancers

Asako Ooe · Kikuya Kato · Shinzaburo Noguchi

Received: 26 May 2006 / Accepted: 30 May 2006 / Published online: 5 July 2006

Abstract
Background Present study was aimed to investigate the relationship of p53 mutation status with response to docetaxel in breast cancers. In addition, attempts were made to identify the genes differentially expressed between p53-wild and p53-mutated breast tumors and to study their relationship with response to docetaxel.
Methods Mutational analysis of p53 was done in 50 breast tumor samples obtained from primary breast cancer patients (n = 33) and locally recurrent breast cancer patients (n = 17) before docetaxel therapy. Response to docetaxel was evaluated clinically. Gene expression profiling (n = 2,412) was conducted by adapter-tagged competitive-PCR in 186 tumor samples, which were also analyzed in their p53 mutational status in order to identify the differentially expressed genes according to p53 mutation status and their relationship with response to docetaxel.
Results Response rate of p53-mutated tumors (44%) was lower than that of p53-wild tumors (62%) though there was no statistical significance (P = 0.23). Of 2412 genes, mRNA expression of 13 genes was significantly different between p53-wild and p53-mutated tumors. Of these 13 genes, mRNA expression of CCT5, RGS3, and YKT6 was significantly up-regulated in p53-mutated tumors and associated with a low response rate to docetaxel. Treatment of MCF-7 cells with siRNA specific for CCT5, RGS3, or YKT6 resulted in a significant enhancement of docetaxel-induced apoptosis.
Conclusions CCT5, RGS3, and YKT6 mRNA expressions, which are up-regulated in p53-mutated breast tumors, might be implicated in resistance to docetaxel and clinically useful in identifying the subset of breast cancer patients who may or may not benefit from docetaxel treatment.

Keywords CCT5 · RGS3 · YKT6 · Docetaxel resistance · p53-Mutated tumors in human breast cancers

Abbreviations

ER	Estrogen receptor
RGS3	Regulator of G-protein signaling 3
CCT5	Chaperonin containing TCP1 Subunit 5 (epsilon)
YKT6	Soluble *N*-ethylmaleimide-sensitive-factor attachment protein receptor (SNARE) protein Ykt6
siRNA	Small interfering RNA
DHPLC	Denaturing high performance liquid chromatography
ATAC-PCR	Adapter-tagged competitive polymerase chain reaction

A. Ooe · S. Noguchi (✉)
Department of Breast and Endocrine Surgery, Osaka University Graduate School of Medicine, 2-2-E10 Yamadaoka, Suita, Osaka 565-0871, Japan
e-mail: noguchi@onsurg.med.osaka-u.ac.jp

K. Kato
Osaka Medical Center for Cancer and Cardiovascular Diseases, Research Institute, 1-3-2 Nakamichi, Higashinari-ku 537-8511, Osaka, Japan

Introduction

There are many active anti-tumor drugs for the treatment of breast cancers, and, recently, an increasing

number of breast cancer patients have been treated with chemotherapy in the neoadjuvant, adjuvant, and metastatic settings. It is obvious that chemotherapy has improved the survival in the adjuvant setting [1, 2], increased the feasibility of breast conserving surgery in the neoadjuvant setting [3, 4], and relieved the symptoms and prolonged the survival in the metastatic setting [5]. One of the most important problems in chemotherapy is inability to identify which drug will benefit a particular patient before the start of chemotherapy. It is well established that estrogen receptor (ER) is clinically very useful in the prediction of response to hormonal therapy but, unfortunately, no clinically useful predictive factor for any chemotherapy has been established yet, whereas a lots of preliminary and unconfirmed observations have been reported [6, 7]. It seems to be very important to develop such predictive factors in order to improve the efficiency of chemotherapy.

Docetaxel, which belongs to taxanes, is one of the most active anti-tumor drugs for breast cancer, and is often used in the neoadjuvant, adjuvant, and metastatic settings. The response rate to docetaxel is approximately 50% in the first line chemotherapy for metastatic diseases, and it decreases to be 20–30% in the second or third line chemotherapy [8, 9]. Therefore, it is of vital importance to select the patients who are very likely to respond to docetaxel in order to eliminate the unnecessary treatment. Several markers have been proposed as predictive factors for docetaxel response which include B-cell CLL/lymphoma 2 (Bcl-2) [10, 11], cytochrome P450, family 3, subfamily A, polypeptide 4 (CYP3A4) [12], β-tubulin [13], breast cancer 2, early onset (BRCA2) [14], human epithelial growth factor receptor type 2 (HER2) [15], and tau [16]. Furthermore, recently, Chang et al. [17] have demonstrated that expression profile of the 92 genes selected using the Affymetrix microarrays is useful in the prediction of a response to docetaxel in the neoadjuvant setting. We have also shown that the 85 genes selected using adapter-tagged competitive-PCR (ATAC-PCR) can predict a response to docetaxel in the neoadjuvant setting with a high accuracy [18]. However, clinical significant of these proposed predictive factors and diagnostic systems have yet to be established.

It has been suggested from the in vitro studies that docetaxel induces apoptosis of cancer cells through the p53-independent pathway, but p53 status may influence cell-cycle progression following mitotic arrest. Thus, it seems to be interesting to study the relationship between p53 mutation status and response to docetaxel in human breast cancers. A few reports have been available which studies the p53 status by immunohistochemistry and its relationship with response to docetaxel [7, 19]. Although these studies failed to demonstrate a significant association between p53 immunohistochemical status and response to docetaxel, it is still possible that p53 mutation status might show a significant association because immunohistochemistry can not detect all the p53 mutations, and location of p53 mutations might also be important as has been suggested from the study on the impact of location of p53 mutations on doxorubicin resistance, i.e., p53 mutations in the zinc finger domains, but not in the other regions, are associated with doxorubicin resistance [20, 21]. Thus, it is very important to investigate the p53 mutation status as well as its association with a response to docetaxel. In addition, it seems to be interesting to find out the genes differentially expressed between p53-mutated and p53-wild breast tumors and to investigate the significance of expression of such genes as a predictor of response to docetaxel.

Therefore, in the present study, firstly, we studied the relationship between the p53 mutation status and a response to docetaxel in the neoadjuvant setting, and, secondly, we selected the genes which were differentially expressed between p53-mutated and p53-wild breast tumors by gene expression profiling (ATAC-PCR), and studied the association of expression of such genes with a response to docetaxel.

Experimental procedures

Tissue specimens

Fifty female patients with primary invasive (n = 33) or locally recurrent (n = 17) breast cancers who were scheduled to be treated with docetaxel were recruited in this study. Tumor samples were obtained from primary breast tumors or locally recurrent lesions by incisional biopsy or vacuum-associated core needle biopsy, and, then, docetaxel (60 mg/m^2 i.v. every 3 weeks) was given to the patients with primary breast tumors at four cycles before surgery and to those with recurrent tumors until disease progression. No patients had been treated previously with taxanes before the recruitment in this study. Informed consent as to the study was obtained from all patients.

Tumor samples were also obtained for mutational analysis of p53 and for identification of the differentially expressed genes between p53-wild and p53-mutated tumors from the other 136 breast cancer patients (96 primary breast cancer patients and 40 locally

recurrent breast cancer patients) who were treated during the period of 1998–2000. Tumor samples were snap-frozen in liquid nitrogen and stored at –80°C until use. Total RNA and genomic DNA were extracted from frozen tissues using TRIZOL reagent (Molecular Research Center, Cincinnati, OH) and the standard phenol/chloroform and ethanol precipitation–extraction procedure, respectively.

Evaluation of response to docetaxel

Chemotherapeutic response was evaluated after four cycles of treatment or at the time when disease progressed according to the WHO clinical criteria: complete response (CR), disappearance of all known disease; partial response (PR), 50% or more decrease in tumor size; no change (NC), less than 50% decrease or less than 25% increase in tumor size; and progressive disease (PD), 25% or more increase in tumor size or appearance of new lesions. Patients showing CR or PR were considered as responders, and those showing NC or PD were considered as non-responders.

Sequence-based analysis of p53 status

Tumor samples obtained from the 50 patients before docetaxel therapy and from the other 136 patients were subjected to mutational analysis of p53. We sequenced the entire open reading frames of p53 (exons 2–11). PCR amplifications were performed using the TAKARA Ex Taq System (Takara, Shiga, Japan) according to the manufacture's protocol. Primers were designed according to the p53 sequence gene bank (Accession No. AY838896) and the respective sequences of primers are given in Table 1. Mutation screening was performed using denaturing high performance liquid chromatography (DHPLC) as described [22, 23]. A WAVE DNA-Fragment Analysis System (Transgenomic Inc. Omaha, NE) was used. All DHPLC positive signals were confirmed by conventional method. Sequencing reactions were performed using the Applied Biosystems Dye-Terminator Kit and analyzed on an ABI Prism 310 DNA sequencer (Applied Biosystems, Foster City, CA).

ATAC-PCR analysis and real-time quantitative PCR

The ATAC-PCR analysis of 2,412 genes mRNA expression was performed on tumor samples according to the method previously described [24]. The protocols and information on the genes analyzed by ATAC-PCR in the present study are available at http://genome.mc.pref.osaka.jp. Real-time PCR reactions were carried out using SYBER Green (Applied Biosystems). Levels of β-glucuronidase mRNA were quantified as an internal standard. The PCR products were detected using an ABI PRISM 7700 Sequence Detection System (Applied Biosystems). Primers were designed using the ABI Primer Express software to cross an exon/exon boundary to minimize the chance that a signal was from contaminating DNA. PCR reactions performed in duplicate for each sample and the mean value at which the PCR product crossed the threshold (Ct) was calculated.

Table 1 Oligonucleotide primer pairs used for mutation analysis, covering the coding region of p53

Exon	Primer name	Nucleotide sequence (5′–3′)	Tm°C
2–3	p53-exon2–3F	tcc tct tgc agc agc cag act gc	66
	p53-exon2–3R	aac cct tgt cct tac cag aac gtt g	
4	p53-exon4F	tgg tcc tct gac tgc tct ttt c	64.5
	p53-exon4R	aag tct cat gga agc cag cc	
5	p53-exon5F	ctc ttc ctg cag tac tcc cct gc	66
	p53-exon5R	gcc cca gct gct cac cat cgc ta	
6	p53-exon6F	gat tgc tct tag gtc tgg ccc ctc	66
	p53-exon6R	ggc cac tga caa cca ccc tta acc	
7	p53-exon7F	gtg ttg tct cct agg ttg gct ctg	66
	p53-exon7R	caa gtg gct cct gac ctg gag tc	
8	p53-exon8F	acc tga ttt cct tac tgc ctc tgg c	66
	p53-exon8R	gtc ctg ctt gct tac ctc gct tag t	
9	p53-exon9F	gcc tct ttc cta gca ctg ccc aac	66
	p53-exon9R	ccc aag act tag tac ctg aag ggt g	
10	p53-exon10F	tgt tgc tgc aga tcc gtg ggc gt	66
	p53-exon10R	gag gtc act cac ctg gag tga gc	
11	p53-exon11F	tgt gat gtc atc tct cct ccc tgc	66
	p53-exon11R	ggc tgt cag tgg gga aca aga agt	

Tm°C: Annealing temperature

Immunohistochemistry

For immunohisotchemical detection of chaperonin containing TCP1, subunit 5 (CCT5), regulator of G-protein signaling 3 (RGS3), and soluble *N*-etylmaleimide-sensitive-factor attachment protein receptor (SNARE) protein Ykt6 (YKT6), paraffin sections were deparaffinized with xylene, and rehydrated using graded ethanol. The sections were incubated in 3% hydrogen peroxide and methanol for 10 min to inactivate endogenous peroxidase. Then, the sections were boiled for 3 min in 10 mM citrate buffer and cooled for 15 min at room temperature for three times to expose antigenic epitopes. Reagents were used as supplied in the Ready-To-Use VECTASTAIN® *Elite* ABC Kit (Vector Laboratories, Burlingame, CA). Sections were incubated for 30 min with goat polyclonal anti-RGS3 (sc-9304; Santa Cruzu Biotechnology, Santa Cruz, CA), (1:1000), rabbit polyclonal anti-TCP-1ϵ (CTA-230; Stress Gen, B.C., Canada), (1:1000) and goat polyclonal anti-v-SNARE Ykt6p (sc-10835; Santa Cruzu Biotechnology), (1:100) at room temperature. Detection was then completed with incubation with a 3,3′-diaminobenzidine solution (Vector Laboratories) diluted in distilled water for 10 min. Finally, the sections were counterstained with hematoxylin, dehydrated, and mounted.

Cell cycle analysis

The human breast cancer cell line MCF-7 was purchased from the American Type Culture Collection (Manassas, VA). The cells were maintained in Dulbecco's modified Eagle's medium (Sigma, ST. Louis, MO) supplemented with 10% fetal bovine serum (Gibco BRL, Carlsbad, CA) and incubated at 37°C in 5% CO_2. Cell cycle distribution was analyzed using a FACScan apparatus (BD biosciences, Franklin Lakes, NJ). MCF-7 cells were treated with various concentrations of docetaxel, for 24 h or 48 h. Cells were then trypsinized, washed with PBS twice and resuspended after removal of trypsin of DNA dye containing 50 μg/ml propidium iodide (Sigma), 0.1% sodium citrate (Wako, Osaka, Japan), 0.1% NP-40 (Wako) and 4 mM EDTA (Sigma). Cells were incubated at 4°C for 12 h, and then analyzed on a FACScan using CellQuest (BD bioscience) acquisition software. List mode data were acquired on a minimum of 2×10^4 single cells. The percentage of cells in different cell cycle phases was calculated using ModFit LT for Mac (BD bioscience).

Small interference RNA (siRNA) transfection

For the siRNA studies, a smart pool of double-stranded siRNA against RGS3, CCT5, or YKT6 as well as non-functioning siRNA were obtained from Dharmacon Tech (Lafayette, CO) and used according to the manufacturer's instructions. MCF-7 cells were seeded in six-well plates or 4-well Lab-Tek Chamber slides (Naloge Nunc International, Rochester, NY) and allowed to adhere overnight until 70–80% confluent. The next day, cells were transfected with siRNA using the oligofectamine protocol (Invitrogen, Carlsbad, CA) as described [25]. The final concentration for the siRNAs was 50 nM. Twenty-four hours after transfection the cells were treated with 10 nM docetaxel (LKT Laboratories, St. Paul, MN). After 24 h of treatment, the adherent cells were collected for either Western blot analysis, or another assays.

Western blot analysis

At 48 h after siRNA transfection, cells were harvested and subjected to protein immunoblot analysis. Cell were washed once with cold PBS and collected by scraping in lysis buffer (10 mM Tris–HCl, pH 7.4, 150 mM NaCl, 1% SDS, 0.12% Triton X, 1 mM EDTA, and protease inhibitor cocktail (Sigma)) and cleared by centrifugation. Protein concentration was determined using Bio-Rad protein assay (Bio-Rad, Hercules, CA). Equal amounts of total protein were then separated using SDS-PAGE, electro-transferred onto Hybond™-P membranes (Amersham, Bucks, UK). Membranes were incubated with specific antibodies recognizing CCT5 (1:2,000), RGS3 ($1:2 \times 10^4$), and YKT6 (1:5,000). The results were visualized with chemiluminescence using ECL Plus™ detection reagents (Amersham). Band intensities were determined by a scanning laser densitometer.

Apoptosis assay

Apoptotic cells were confirmed with the DeadEnd™ Fluorometric TUNEL System (Promega, Madison, WI), in accordance with the manufacturer's instructions. Cells were grown on chamber slides. The next day, cells were transfected with siRNAs. At 24 h after transfection, cells were treated with 10 nM docetaxel for 24 h. Slides with adherent cells were fixed in 4% paraformaldehyde for 25 min at 4°C and permiabilized with 0.2% Triton X-100 for 5 min at room temperature. Free 3′ ends of fragmented DNA were enzymatically labeled with the TdT-mediated dUTP nick end labeling (TUNEL) reaction mixture for 60 min at 37°C

in a humidified chamber. Labeled DNA fragments were monitored by fluorescence microscopy. Ten fields were randomly counted for each sample.

Results

Relationship between p53 mutation and response to docetaxel

Of 50 tumors obtained before docetaxel therapy, 16 were found to have somatic mutations including 7 missense mutations, 3 nonsense mutations, and 6 frameshift mutations. Relationship between p53 mutation status and response to docetaxel is shown in Table 2. Response rate of tumors with mutated p53 (44%) was lower than tumors with wild p53 (62%) though there was no statistical significance ($P = 0.23$). Of 16 tumors with p53 mutation, 9 tumors had mutations in the L2/L3 regions. Response rate of tumors with p53 mutation in these regions were lower, though not statistically significant, than the other tumors (33% vs. 61%).

Identification of differentially expressed genes between p53-wild tumors and p53-mutated tumors

In total, 186 tumor samples were analyzed in the p53 mutational status (Table 3) as well as the 2,412 genes mRNA expression profile. These tumor samples were divided into the first set ($n = 90$) and the second set ($n = 96$). The first set consisted of 67 p53-wild tumors and 23 p53-mutated tumors and the second set consisted of 74 p53-wild tumors and 22 p53-mutated tumors. Differentially expressed genes between p53-wild tumors and p53-mutated tumors were selected by permutation test with a statistical significance of $P < 0.05$ in each set, and, finally, 13 genes were found to be differentially expressed with a statistical significance ($P < 0.05$) in both sets (Table 4).

Table 2 Relationship between p53 mutation status and response to docetaxel

	Responders	Non-responders	
p53 mutation status			
p53-mutated tumors	7	9	
p53-wild tumors	21	13	$P = 0.23$
p53 mutation status			
p53-mutated (L2/L3) tumors	3	6	
Other tumors[a]	25	16	$P = 0.13$

[a]Including p53-wild tumors and p53-mutated (outside L2/L3) tumors

Relationship of mRNA levels of differentially expressed 13 genes between p53-wild tumors and p53-mutated tumors with response to docetaxel

The mRNA expression levels of the 13 genes differentially expressed between p53-wild tumors and p53-mutated tumors were further analyzed by a real-time PCR assay which is considered to be currently the most reliable method for quantification of mRNA levels, and their relationship with response to docetaxel was evaluated. Finally, of these 13 genes, three genes including chaperonin containing TCP1, subunit 5 (CCT5), regulator of G-protein signaling 3 (RGS3), and soluble *N*-etylmaleimide-sensitive-factor attachment protein receptor (SNARE) protein Ykt6 (YKT6) were found to be differentially expressed between responders and non-responders with a statistical significance (Fig. 1).

Expression of CCT5, RGS3, and YKT6 in breast cancers

Immunohistochemical staining of CCT5, RGS3, and YKT6 using the representative tumor samples revealed that all of them were predominantly localized in tumor cells. From the viewpoint of subcellular localization, YKT6 was exclusively localized in the cytoplasm of tumor cells, and CCT5 and RGS3 were predominantly localized in the nucleus with a concomitant cytoplasmic staining of various intensities (Fig. 2).

Effect of docetaxel on cell cycle

Effect of various concentrations of docetaxel on MCF-7 cell cycles was studied by flow cytometry (Fig. 3). There was no significant difference in flow cytometric pattern at 1 nM or lower concentrations but the percentage of cells in G_0/G_1 phase apparently decreased and that in the sub-2N apparently increased at 5 nM or higher concentrations, suggesting the presence of apoptosis induced by docetaxel. From these results, we chose 10 nM docetaxel for the further investigation.

Influence of knock-down of CCT5, RGS3, and YKT6 mRNA by siRNA on sensitivity to docetaxel in MCF-7 cells

For the purpose of validating the involvement of CCT5, RGS3, and YKT6 in resistance to docetaxel, we next studied the influence of knock-down of the endogenous CCT5, RGS3, and YKT6 expression by siRNA on sensitivity to docetaxel in MCF-7 cells. CCT5, RGS3, or YKT6-specific siRNAs were transfected into MCF-7

Table 3 Summary of p53 mutations found in 186 breast tumors

Type of variation	Exon	Nucleotide change	Protein change	Frequency
Missense mutation	2–3	1174 g to c	11 Glu to Gln	1
	4	12256 t to c	111 Leu to Pro	1
	6	13341 t to g	194 Leu to Arg	1
		13374 a to c	205 Tyr to Ser	1
		13405 t to g	215 Ser to Arg	1
		13418 t to a	220 Tyr to Asn	3
	7	14061 g to t	245 Gly to Val	1
		14069 c to t	248 Arg to Try	2
		14070 g to a	248 Arg to Gln	4
		14097 t to a	257 Leu to Gln	1
	10	17593 g to c	339 Glu to Gln	1
		17657 g to c	360 Gly to Val	1
	11	18673 c to t	392 Ser to Leu	1
Stop codon	4	12108 g to t	62 Glu to Stop	1
	5	13227 c to g	183 Ser to Stop	1
	6	13346 c to t	196 Arg to Stop	1
	10	17602 c to t	342 Arg to Stop	5
Deletion out-of-frame	5	1 bp deletion		1
		4 bp deletions		1
		20 bp deletions		1
	6	1 bp deletion		1
		2 bp deletions		1
		14 bp deletions		1
	7	1 bp deletion		1
		2 bp deletions		1
	8	1 bp deletion		1
		10 bp deletions		1
		20 bp deletions		1
		26 bp deletions		2
Insertion out-of-frame	4	1 bp insertion		3
	8	1 bp insertion		1
		17 bp insertions		1
Polymorphism	4	12032 g to a	32 Pro to Pro	2
		12139 g to c	72 Arg to Pro	3

cells and CCT5, RGS3, or YKT6 protein levels were determined by Western blotting. CCT5-, RGS3-, and YKT6-specific siRNA suppressed the CCT5, RGS3, and YKT6 protein levels by 90%, 40%, and 60%, respectively, in MCF-7 cells (Fig. 4). The inhibitory effect of each siRNA was considered to be specific because transfection with non-specific siRNA did not significantly alter the expression of each gene. CCT5 protein levels, but not RGS3 and YKT6 proteins, showed a significant increase as compared with non-specific siRNA transfected cells after the treatment with docetaxel.

Table 4 List of 13 genes differentially expressed between tumors with wild p53 and mutated p53

Clone ID	PRI	Definition	Expression in p53-mutated tumors
GS6451	AB028641	SRY (sex determining region Y)-box 11	↑
GS5078	AL050337	Interferon gamma receptor 1	↓
GS4467	X06323	Mitochondrial ribosomal protein L3	↑
GS7542	AL121961	Stromal membrane-associated protein 1	↓
GS3966	BC002971	Chaperonin containing TCP1, subunit 5 (epsilon)	↑
GS3957	AA193183	SNARE protein Ykt6	↑
GS6282	BC003667	40s ribosomal protein S27 isoform	↓
GS6864	BC000382	Interleukin enhancer binding factor 2	↓
GS6703	BC002460	Programmed cell death 9	↓
GS5014	U27655	Regulator of G-protein signaling 3	↑
GS3885	BC000672	Guanine nucleotide binding protein, beta polypeptide2-like1	↓
GS4530	BC003162	Lamin A/C	↑
GS6473	BC001929	Hypothetical protein MGC2376	↓

PRI: GenBank Accession No.

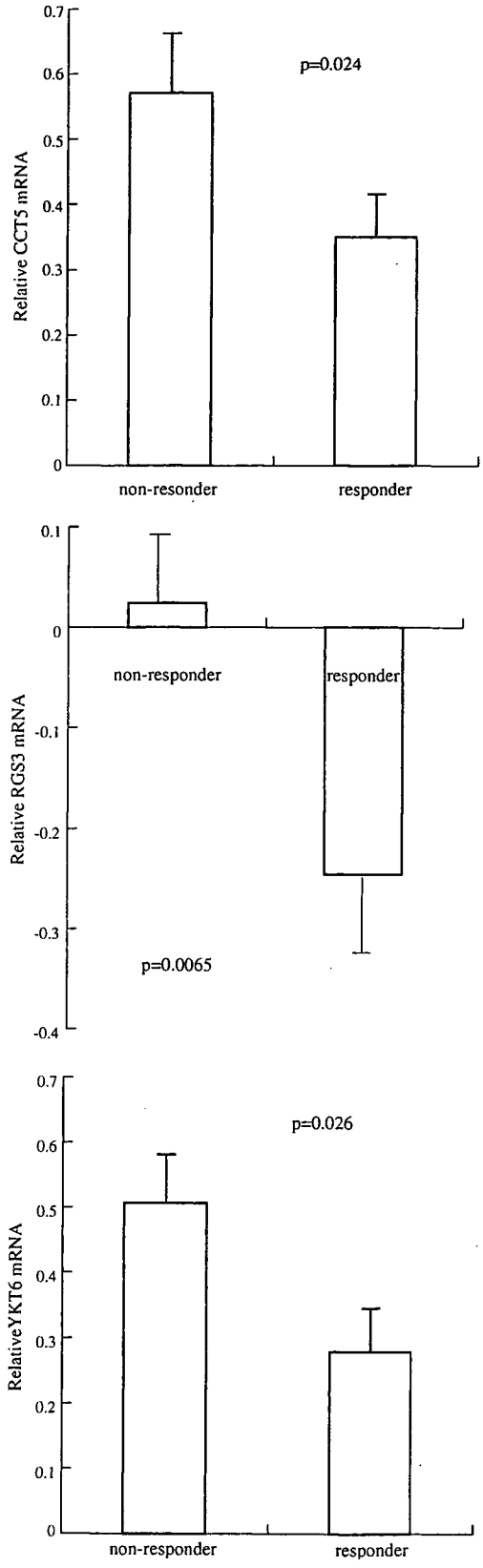

Fig. 1 Relationship of mRNA expression of CCT5, RGS3, or YKT6 with response to docetaxel. Bars; mean ± SE

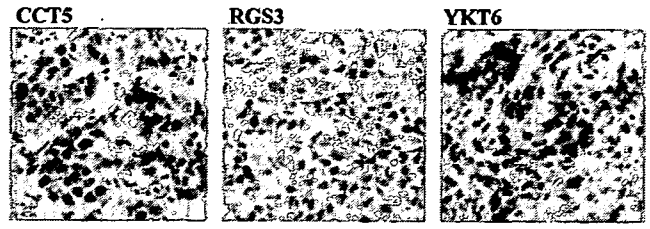

Fig. 2 Immunohistochemical study on CCT5, RGS3, and YKT6 in breast cancers (×200)

Effect of siRNA treatment on sensitivity to docetaxel was evaluated by apoptotic index determined by TUNNEL assay in MCF-7 cells. As shown in Fig. 5, transfection of CCT5-, RGS3-, and YKT6-specific siRNA showed a significant increase (6.6%, 8.6 %, and 8.1%, respectively) in apoptotic index after docetaxel treatment.

Discussion

Since p53 plays an important role in the induction of apoptosis and several in vitro studies have suggested that p53-apoptotic pathway might be involved in the anti-tumor activity of docetaxel, the relationship between p53 mutation status and response to docetaxel therapy has been investigated in the clinical settings by several investigators [7, 19]. These studies, however, failed to show a significant association between p53

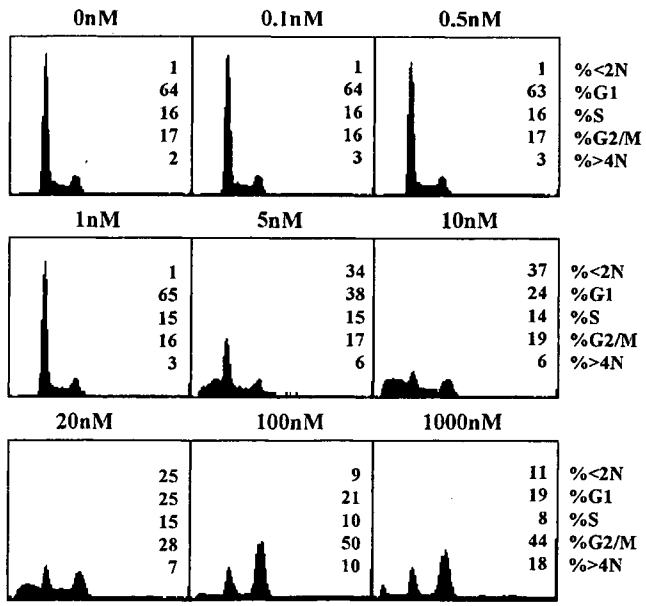

Fig. 3 Influence of docetaxel on cell cycle. MCF-7 cells were treated with various concentrations of docetaxel for 24 h and analyzed by flow cytometry. The percentages of cells in each phase of the cell cycle (sub 2N, G_0/G_1, S and G_2/M) are shown

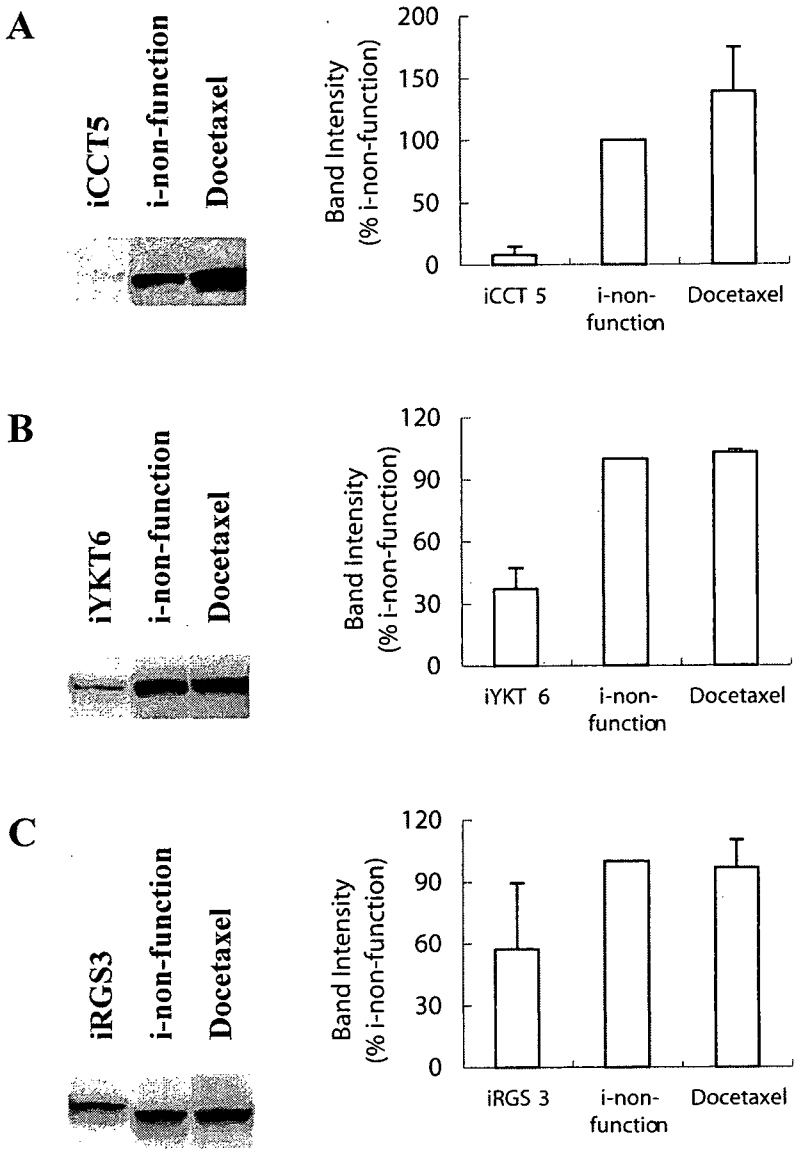

Fig. 4 Influence of siRNA transfection on CCT5, YKT6, and RGS3 protein levels in MCF-7 cells. Cells were transfected with siCCT5, siYKT6 or siRGS3, and CCT5 (panels A), YKT6 (panels B), or RGS3 (panels C) protein level was determined by Western blot analysis with treatment of 10 nM docetaxel for 24 h. Bars; mean ± SD of triplicate determinations

mutation status and response to docetaxel. In all of these studies, p53 mutation status was evaluated by immunohistochemistry, which is a less reliable method than mutational analysis of genomic DNA. Immunohistochemistry can detect missense mutation but not the other types of mutations including nonsense and frameshift mutations. Thus, in the present study, we have analyzed the p53 mutation status of genomic DNA in entire coding regions (exons 2–11). The frequency of p53 mutations was 24% (45/186) in our study, which is in accordance with the most published reports [26, 27]. Of these 45 mutations, as many as 26 mutations (58%) were nonsense mutations (8) or frameshift mutations (18), both of which are unable to be detected by immunohistochemistry. Although, in most studies, mutation analysis of p53 is limited to the hotspots (exons 5–8), we analyzed the entire coding exons 2–11 in the present study. Of the 45 mutations, 14 (31%) were located outside of the exons 5–8, indicating that almost 1/3 of mutations would have been overlooked if we had limited the analysis to the exons 5–8. These results clearly demonstrate that analysis of the entire coding exons is very important to elucidate the mutation status of p53. We have found that p53-wild breast tumors show a slightly higher response rate (62%) than p53-mutated breast tumors though there was no statistical significance. Since breast tumors with p53 mutations in the L2/L3 loop domains have been reported to show a strong resistance to doxorubicin, we have also studied the relationship between p53 mutations in L2/L3 and response to docetaxel. Nine breast tumors (56%) were found to have mutations in L2/L3. Their response rate (33%) was lower than that of the other breast tumors (61%) though, again, statistically